Hindawi Publishing Corporation
Journal of Nanoparticles
Volume 2013, Article ID 672059, 24 pages
http://dx.doi.org/10.1155/2013/672059

Review Article

Recent Advancement in Functional Core-Shell Nanoparticles of Polymers: Synthesis, Physical Properties, and Applications in Medical Biotechnology

K. Santhosh Kumar,[1] Vijay Bhooshan Kumar,[1] and Pradip Paik[1,2]

[1] *Nanoscience and Technology, School of Engineering Sciences and Technology, University of Hyderabad, Hyderabad, Andhra Pradesh 500046, India*
[2] *Materials Engineering, School of Engineering Sciences and Technology, University of Hyderabad, Hyderabad, Andhra Pradesh 500046, India*

Correspondence should be addressed to Pradip Paik; pradip.paik@gmail.com

Received 13 December 2012; Accepted 3 February 2013

Academic Editor: John Z. Guo

Copyright © 2013 K. Santhosh Kumar et al. This is an open access article distributed under the Creative Commons Attribution License, which permits unrestricted use, distribution, and reproduction in any medium, provided the original work is properly cited.

This paper covers the core-shell nanomaterials, mainly, polymer-core polymer shell, polymer-core metal shell, and polymer-core nonmetal shells. Herein, various synthesis techniques, properties, and applications of these materials have been discussed. The detailed discussion of the properties with experimental parameters has been carried out. The various characterization techniques for the core-shell nanostructure have also been discussed. Their physical and chemical properties have been addressed. The future aspects of such core-shell nanostructures for biomedical and various other applications have been discussed with a special emphasis on their properties.

1. Introduction

The core-shell nanomaterials and nanostructures (Figure 1) have become an important research area since few decades due to their potential applications in various fields like catalysts, industrial and biomedical applications, and so forth [1–12].The core-shell nanocomposites and nanostructure may be with different sizes and different shapes of core and shell thickness with different surface morphology. They may be spherical, centric, eccentric, star-like, or tubular in shape. Depending on the size and shape, their properties tune from material to another. Individual core-shell nanoparticles have various applications in diverse fields of medical biotechnology, like molecular bioimaging, drug delivery, cancer therapy, and so forth. Whenever the surface of the nanoparticles is modified by functional groups or molecules or coated with a thin layer of other materials (with different constituents), they show enhanced properties compared to the nonfunctionalized uncoated particles. There are different types of core-shell structure, like (1) metal-core and different metal shell, (2) metal-core and nonmetal shell, (3) metal-core and polymer shell, (4) nonmetal-core and nonmetal shell, (5) polymer-core and nonmetal shell and (6) polymer-core and polymer shell where the two polymers are different. For these six categories, the core and the shell materials may be reversed. Below is the schematic of core-shell nanoparticles.

Recently, much attention has been focused on core-shell metal nanoparticles based on gold, platinum, and palladium because their properties markedly differ from their bulk [1]. These metal core-shell nanoparticles exhibit size-induced quantum-size effects (i.e., electron confinement and surface effect) [1, 2] and can be exploited for a number of advanced functional applications as sensors, electronics, optoelectronics and catalysis [3–5]. Polymer and semiconductor core-shell have attracted considerable interest as a class of new materials with applications in various electronics including organic light-emitting diodes (OLEDs), organic photovoltaics (OPVs), sensors, and organic field effect transistors (OFETs) due to their advantages, such as low cost and easy device fabrication abilities [6–9]. The design and

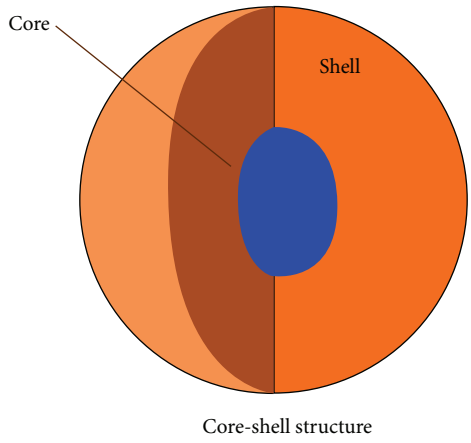

Figure 1: Schematic of a core-shell nanoparticle.

synthesis of novel core-shell nanomaterials/nanostructures with polymers, that possess high mobility, are one of the major challenges in polymer semiconductor research [10–12].

These core-shell nanoparticles are produced by various synthesis approaches like hydrothermal synthesis, solvothermal synthesis, sol-gel method, emulsion polymerization, microemulsion polymerization, and so forth. On the basis of the core and shell of the materials, the synthesis techniques, their properties, and morphologies can be modified.

2. Synthesis and Characterization of Various Types of Core-Shell Nanomaterials

The synthesis, characteristics, and new properties of different core-shell nanomaterials with polymer as either core or shell are summarized in Table 1.

2.1. Polymer-Polymer Core-Shell Nanoparticles and Nanostructure. Functional core-shell polymer nanoparticles and nanocomposites have attracted a lot of attention due to the special thermal, mechanical, and electrical properties [53]. Significant improvement of properties can often be achieved at a very low nanoparticle volume fraction. A water-soluble fluorescent hyperbranched conjugated polyelectrolyte (HCPE) with a unique double-layered architecture has been synthesized via the combination of alkyne polycyclotrimerization and alkyne-azide "click" reaction for live-cell imaging [54]. A number of important synthesis methods of core-shell nanoparticles/nanostructure have been discussed in the subsequent section. Han et al. have synthesized polyaniline-coated poly(butyl methacrylate) core-shell nanoparticles and formulated into electrically conductive colloidal inks appropriate for use in roll-to-roll printing (Figure 2).

The initial phase of the core-shell synthesis was the emulsion polymerization of poly(butyl ethacrylate) particles with a particle size between 100 and 300 nm [50]. The observed particle diameter from transmission electron microscopy (TEM) was 199 ± 4 nm. The observed Mw of the colloidal particles was 221 Dalton and the polydispersity index (PDI) was 2.08. The second step in the core-shell synthesis is to coat the PBMA particles with polyaniline. To protect the PBMA particles from flocculation in the low pH synthetic conditions, poly(N-vinylpyrrolidinone) (PVP, Mw = 360 000), a polymeric stabilizer, was dissolved into the suspension and allowed to be absorbed onto the particles. The resulting core-shell particles were purified by centrifugation. Zhang et al. have synthesized dextran grafted with Poly(N-isopropyl acrylamide-co-N,N-dimethyl acrylamide) (dextran-g-poly (NIPAAm-co-DMAAm)) [51]. The first step was synthesis of the poly(NIPAAm-co-DMAAm) with a methyl ester end group (STP-$COOCH_3$). The polymerization reaction was carried out by free radical copolymerization. Then, Fe_3O_4 nanoparticles were encapsulated with this biodegradable thermosensitive polymer (Figure 3).

As Dextran-g-poly (NIPAAm-co-DMAAm) thermosensitive polymer contains the active 4-nitrophenyl chloroformate groups, they can be cross-linked by 1,6-diaminohexane around the magnetic core to form the core-shell structure (Figure 3) [51]. On the basis of the behavior, the concept of synthesis and the schematic illustration of the experimental procedure of magnetic carrier coated with smart polymer are schematically depicted in Figure 4 [51].

Yuan and Wicks have prepared thermotropic color-changing core-shell nanoparticles through the polymerization technique [55]. Water-dispersed thermotropic nanoparticles with core-shell structures were synthesized by the in situ polymerization of a lightly cross-linked shell of poly(N-isopropyl acrylamide) (poly (NIPAM)) onto blue polystyrene cores. At room temperature poly(NIPAM) hydrophilic in nature and is in a fully swollen gel state. As the temperature is raised beyond 31°C, poly(NIPAM) becomes hydrophobic and eventually collapses as the temperature reaches the lower critical solution temperature (LCST) [55].

2.2. Polymer-Metal Core-Shell Nanoparticles/Nanostructure. Wang et al. synthesized Au-impregnated polyacrylonitrile (PAN)/polythiophene (PTH) core-shell nanofibers and showed improved semiconducting properties like mobility [38]. Tian et al. have designed the self-assembled colloidal core-shell nanoparticles with polystyrene as core and gold nanoparticles as shell [40]. The application of these core-shell-structured colloidal particles to protein separation is also investigated in this research work. Colloidal particles with polystyrene-(PS) coated magnetic nanoparticles in the core were also prepared by this strategy [40]. Hydrophilic citrate-stabilized AuNPs were dispersed in water, and PS with thiol terminal groups (PS-SH) was dissolved in toluene. A stable emulsion was obtained by mixing two solutions via sonication. In the emulsion, AuNPs were located at a liquid-liquid interface. Colloidal particles with PS cores and AuNP coronae were prepared by adding the emulsion to excess methanol. The colloidal particles were stabilized by hydrophilic AuNPs in the coronae. Initially, PS-SH/PS-coated Fe_3O_4NPs were dissolved (or dispersed) in toluene, and then colloidal particles with PS/Fe_3O_4NPs in the cores and AuNPs in the coronae were prepared by a similar strategy (Figure 5).

The weight ratio of PS-SH to AuNP plays an important role in controlling of the morphology of colloidal particles.

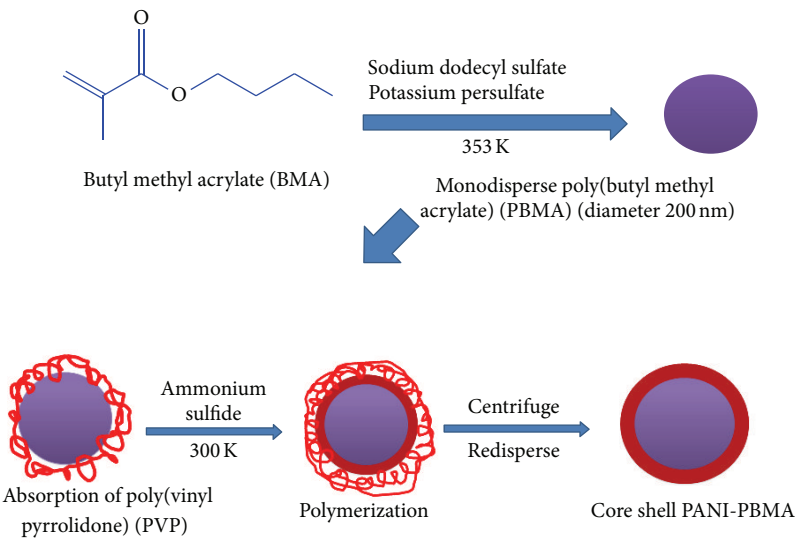

FIGURE 2: Schematic representation showing the proposed synthesis approach of polyaniline-poly(butyl methacrylate) core-shell nanoparticles for using in colloidal inks in flexographic printing.

Figures 6(a)–6(d) show TEM images of various colloidal particles prepared through this method. These colloidal particles do not change after the solvent was changed from methanol to water (Figure 6(f)) [40].

Ohnuma et al. explained that the eccentric structural metal polymer hybrid colloidal particles can be synthesized by precipitation polymerization [46]. Introducing the metal colloids after a few minutes of starting (instead of introducing before) polymerization results in an eccentric structure. The uniform-sized hybrid nanoparticles contain only one metal particle as it is shown in Figure 7.

Xuan et al. synthesized Fe_3O_4@polyaniline@Au core-shell nanocomposites via ultrasound-assisted in-situ surface polymerization [47]. The Fe_3O_4 core material is super paramagnetic in nature and these core-shell nanoparticles can be easily separated from the solution. These core-shell nanoparticles can be used as magnetically recoverable nano catalyst for the reduction of selected substrate. Negatively charged Au nanoparticles can be added on the surface of the Fe_3O_4@polyaniline core-shell microspheres via electrostatic attraction. They have also mentioned the synthesis of Fe_3O_4@PANI nanocomposite with core-shell nanostructures by using PVP (50 mg), and Fe_3O_4 microspheres were dispersed in H_2O under ultrasonication at room temperature. They have also synthesized the Fe_3O_4@PANI@Au core-shell nanocomposites by an electrostatic attraction method. A special effort was employed for the immobilization of Au nanoparticles onto the Fe_3O_4@PANI core-shell microspheres to form the Fe_3O_4@PANI@Au microspheres (Figure 8).

Meredith et al. have synthesized PS bead covered by 30 nm AuNPs and studied the surface morphology through AFM [42]. The metal coating can be formed with homogeneous distribution of AuNPs (Figure 9(a)). AFM images also indicated that the 30 nm AuNP coating consisted of 1 to 3 dense NP layers (Figure 9(b)).

Without the addition of the surfactant, Au/poly(toluidine) core-shell nanoparticles (Au@POT) have been synthesized through chemical polymerization route by Han et al. using $HAucl_4$ [58]. Concentration of oxidant tunes the amount of Au nanoparticles (ten to one) inside each POT sphere with extremely low concentration of oxidant POT hollow spheres with one opening in each polymer surface that can be obtained. Wen et al. synthesised metal nanoparticles embedded in the shell layer of core-shell poly(styrene-co-4-vinylpyridine) microspheres for catalytic applications. By the selective immobilization of noble metal nanoparticles (Pd, Au and Ag) into the shell, the catalytic activity can be increased in noble metal (Pd, Au, and Ag)@polystyrene co-4-vinyl pyridine core-shell microspheres. It contains core of polystyrene and coordinative shell of poly(4-vinyl pyridine) [59]. They synthesized the Pd nanoparticles embedded in the shell layer of core-shell PS-co-P4VP microspheres (PS-co-P4VP-Pd) and the Au and Ag nanoparticles embedded in the shell layer of core-shell PS-co-P4VP microspheres (PS-co-P4VPAu and PS-co-P4VP-Ag) in water. Zhang et al. have reported the synthesis and properties of Fe_3O_4/polypyrrole/Au nanocomposites with core-shell structure [52]. The Au colloids with an average diameter of 15 nm were prepared via deoxidizing $HAuCl_4$ aqueous solution with sodium citric acid. Fe_3O_4/PPy core-shell nanocomposites solution was added to the Au colloid under stirring. The AuNPs are electrostatically attracted to the surface of Fe_3O_4/PPy nanocomposites, leading to formation of Fe_3O_4/PPy/Au core-shell nanocomposites. With the increase of reaction time, the wine red solution turned colorless, adding Au colloids until the color no longer changed, and the resultant product was removed from the solution by applying an external magnetic field and dried (Figure 10).

2.3. Polymer-Nonmetal Core-Shell Nanoparticles/Nanostructure. Rong et al. synthesized PSBM@silica core-shell NPs by emulsion polymerization method [15]. To achieve the core-shell, the surfaces of the silica particles were modified

Table 1: Various synthesis approaches and applications of few important core-shell nanoparticles with polymer.

Sl. no.	Materials	Synthesis method	Properties/uses	Average size of Core-shell particle	References
1	Carbon black/polypyrrole	In situ chemical oxidative polymerization	Electrochemical energy storage	50–100 nm	[13]
2	$BaTiO_3$/PMMA	In situ atom transfer radical polymerization (ARTP)	High dielectric constant materials with the inherent low loss of the base polymer	150–200 nm	[14]
3	Polystyrene-n-butyl acrylate-methy methacrylate@silica	Emulsion polymerization	Dynamic modulus	30–80 nm	[15]
4	Poly(vinyl amine)-silica	Wet chemical route	Silica precursor for composite materials formation	200–250 nm	[16]
5	Silica@PMMA brush	Surface initiated photopolymerization	PMMA composite with enhanced thermal and mechanical properties	100–150 nm	[17]
6	CdS@PMMA	Different physical and chemical routes	Electrical transport properties	10–200 nm	[18]
7	Spiropyran-silica	Two-step sol-gel synthesis	Photochromic properties	100–150 nm	[19]
8	(MMA@CuO)	Solution deposition method	—	20–30 nm	[20]
9	Well-defined oxide (SiO_2) core-polymer (PMMA) shell	Chemical route	High mechanical strength	20–90 nm	[21]
10	T-ZnO whiskers/Polyaniline	Graft polymerization	Electrical conductivity	500 nm	[22]
11	PS cores and thermosensitive poly(N-isopropylacrylamide) (PNIPA) shells	Self-assembly encapsulation	Drug diffusion	Less than 100 nm	[23]
12	Silica-polymer (methyl methacrylate (MMA)) core-shell nanoparticles	Seed copolymerization	Excellent antimicrobial	20–30 nm	[24]
13	PMMA@PCL	Coaxial electrospraying	—	3–6 μm	[25]
14	PS@SiO_2	Sol-gel synthesis	—	200–250 nm	[26]
15	Fe_3O_4@styrene/butyl acrylate	Initiator free miniemulsion polymerization	Magnetite and their corresponding behavior	150–200 nm	[27]
16	Polyaniline-polystyrene sulfonate@Fe_3O_4	Surface-initiated polymerization	Conductive and magnetic properties	60–200 nm	[28]
17	SiO_2@polypyrrole	In situ polymerization through electrostatic interaction	—	200–300 nm	[29]
18	PMMA spheres with a core of Fe_3O_4	Spontaneous Pickering emulsification	—	50–80 nm	[30]
19	PS@SiO_2	Alcaholic dispersion polymerization	Catalytic	1000 nm	[31]
20	Poly(2-vinylpyridine) @silica	Emulsion polymerization	Cationic azo initiator	200 nm	[32]
21	SiO_2@Poly(3-aminophenylboronic acid) (PABBA)	Ultrasonic irradiation method	Conductivity	100–200 nm	[33]
22	Collagen-g-PMMA Ag@TiO_2 Collagen-g-PMMA@TiO_2	Graft polymerization water in oil emulsion polymerization ultrasonic irradiation	Lower infrared emissivity	60–100 nm	[34]

Table 1: Continued.

Sl. no.	Materials	Synthesis method	Properties/uses	Average size of Core-shell particle	References
23	SiO_2@polyaniline	In situ polymerization	High electrical conductivity	20–30 nm	[35]
24	PANI@Fe_3O_4	Ultrasonic polymerization to assist chemical oxidative polymerization	Decreases its electrical conductivity	20–25 nm	[36]
25	SiO_x@PAM PAM: polyacrylamide	UV assisted in situ surface initiated free radical polymerization	Good dispersion stability	50–200 nm	[37]
26	Au-impregnated polyacrylonitrile (PAN)/polythiophene (PTH) core-shell nanofibers	Shadow mask	High-performance semiconducting properties	30–50 nm	[38]
27	Smart core-shell hybrid nanogels with Ag nanoparticle core and poly(N-isopropylacrylamide-co-acrylic acid) shell	Copolymerization process	pH-Regulated drug delivery and for cancer cell imaging	40–80 nm	[39]
28	PS cores and Au shell nanoparticle coronae	Self-assembly	Hydrophobic nanoparticles	80 nm	[40]
29	Upconverting $NaYF_4$ nanoparticles with PEG-phosphate ligands	Water-dispersible	Biolabeling within the biological window	30–40 nm	[41]
30	Au@PEG (polyethylene glycol)	Combined swelling heteroaggregation	Dielectric applications	300 nm	[42]
31	Ag-polystyrene	Hydrothermal method	Characteristic plasmon resonance	200 nm	[43]
32	Ag@poly(acrylic acid)	In situ immobilization	Tunable photoluminescence, act as multiple-sensitive hybrid microgels	100 nm	[44]
33	Highly controlled core (Au/shell (PANI) structures	In situ polymerization,	Tunable conductive polymer	61–92 nm	[45]
34	Au-PS hybrid colloidal particles	Precipitation polymerization method	Fabricating photonic devices via a self-assembly approach	200–250 nm	[46]
35	Fe_3O_4@polyaniline@Au Nanocomposites	Solvothermal reaction	Catalytic activity	70–80 nm	[47]
36	Luminescent silver@phenol formaldehyde resin core-hell nanospheres	Facile one-step hydrothermal approach	In vivo bioimaging	180–1000 nm	[48]
37	Poly(butylene adipate) on the surface of SiO_2	Chemical route	Improve the toughness and stiffness	100–1000 nm	[49]
38	Polyaniline-coated poly(butyl methacrylate)	Chemical route	Printing technology	100 nm	[50]

with oleic acid. The addition of silica NPs inhibit the chain movement and increased the moduli, which are strongly dependent on the extent and distribution of silica NPs in PSBM. Annenkov and coworkers found that the degree of polymerization and the pH of organic polymer decide the morphology of the end product (i.e., core-shell nanoparticles (CSNPs) [16]. In the synthesis of poly(vinyl amide@silica), it is observed that only high molecular weight polymer with longer chain length (i.e., degree of polymerization is high) helps to form the core-shell structure. When the degree of polymerization is less than 1000, then the associates of polymer silica core shell form nanostructure. The cooperative interactions of the silica with polymer chains tune the size of the particles with the degree of polymerization and pH. Chen et al. synthesized silica@PMMA core-shell nanoparticles with light-initiated polymerization method [17]. The thickness of

Table 2: Comparison of infrared emissivity values of various samples.

Infrared emissivity values of samples	
Samples	Infrared emissivity (ETIR at 8–14 μm)
Collagen	0.851
Collagen-g-PMMA	0.896
Ag@TiO_2	0.514
Collagen-g-PMMA/Ag@TiO_2	0.496

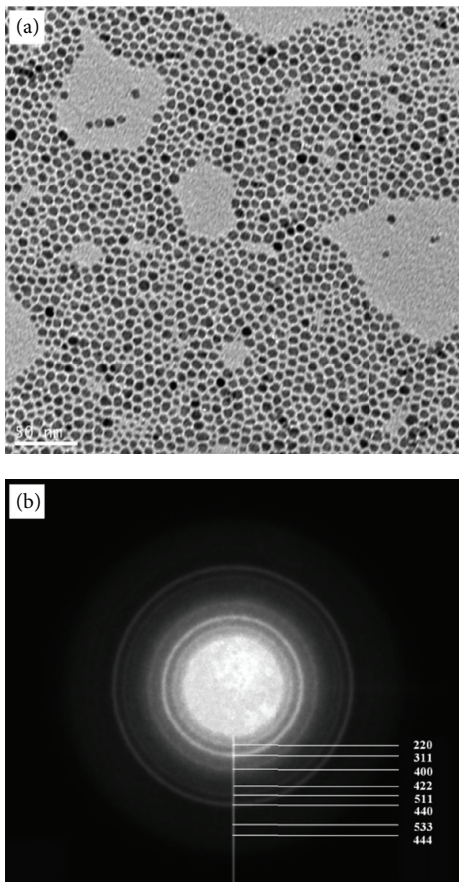

Figure 3: (a) TEM micrograph and (b) selected electron diffraction pattern (SAED) [51].

the PMMA shell can be tuned by UV irradiation (Figure 11) without altering the main chemical structures and bondings of the composite systems [12]. The SiO_2 particles impregnated in the PMMA help to enhance the overall mechanical and thermal properties of the core shell.

Chen and coworkers have also synthesized well-defined PMMA brush on silica particles by surface-initiated photopolymerization (SIPP) [17]. The photochemical method is a convenient and simple route to achieve polymer brush on the surface of a nanoparticle. They synthesized PMMA brush on silica particles (SPs) by the combination of self-assembly monolayer of hyperbranched polymeric thioxanthone (HPTX) and surface-initiated photopolymerization (SIPP). HPTX was immobilized on the surface of silica particles (SPs) through nucleophilic addition between amine and epoxy groups and then initiated photopolymerization of MMA to generate PMMA brush on SPs at room temperature (Figures 12 and 13).

Synthesis of polymer brush on particles by photochemical approach has potential application as a printing ink and is little challenging because of the excellent UV absorbance hypoxanthine [60]. Thioxanthone can absorb UV light (250 nm–350 nm) with a large extent even in the case of pigment particles' shield and is consequently widely used in photocuring systems containing pigment particles such as coating and printing ink [61].

Allouche et al. synthesized hybrid spiropyran-silica nanoparticles with a core-shell structure by sol-gel synthesis having good photochromic properties [19]. Photochromic hybrid spiropyran-silica nanoparticles with a core-shell structure were synthesized via a two-step sol-gel procedure using tetraethoxysilane (TEOS) and methyltriethoxysilane (MTEOS) as silica precursors. The chemical nature and porosity of the materials were modified by the precursor ratio, and the silylated spiropyran derivative chromophore was grafted and confined inside the nanoporous shell producing photoresponsive nanomaterials with a tunable dye photochromic response [19].

Polymer nanoparticles can be coated with silica by the Stober method [62, 63]. In this method, the reaction rates depended on the pH. At low pH the reaction rate is very low. That means there is very thin coating or almost no coating of silica on polymer beads at low pH. But at high pH, thick silica coating with heterogeneous nucleation is observed. Chen et al. have found out that the surface modification of the core material plays an important role in the synthesis of core-shell structures [22]. It also provides enhancement of properties of CSNPs (core-shell nanoparticles). In the synthesis of tetra-needle-like ZnO whiskers (T-ZnOw)@polyaniline core-shell composites, surface modification of T-ZnOw with ATPS amino propyl triethoxysilane results in intactness of the morphology structure of T-ZnOw and provides a surface site for in situ polymerization of the T-ZnOw. These CSNCs showed a higher electrical conductivity than that of the pure T-ZnO.

Polystyrene particles with hollow structure can also be coated with SiO_2 through sol-gel method. Initially, polystyrene latex particles can be synthesized using 4-VP (4-vinylpyridine) as functional comonomer and PVP as surfactant (Figure 14) [26]. The morphology depends on the initial feeding rate of the precursors like 4-VP and PVP.

Core-shell magnetic colloidal particles have potential demand in the fields of nano technology. Fe_3O_4@PS core-shell magnetite nanoparticles can be modified by styrene and butyl acrylate through miniemulsion polymerization [27]. Mahdavian et al. have prepared surface-modified Fe_3O_4 (m-Fe_3O_4) through ultrasonication and polymerization methods [27]. A synthesis method for core shell has been introduced by Lee et al. to achieve PANI-polyaniline-polystyrene sulfonate@Fe_3O_4 (conducting magnetic) core-shell nanoparticles [28]. Each core-shell particle has single Fe3O4 (magnetic) particle and the polymer shell evenly encapsulated the core (Figure 15).

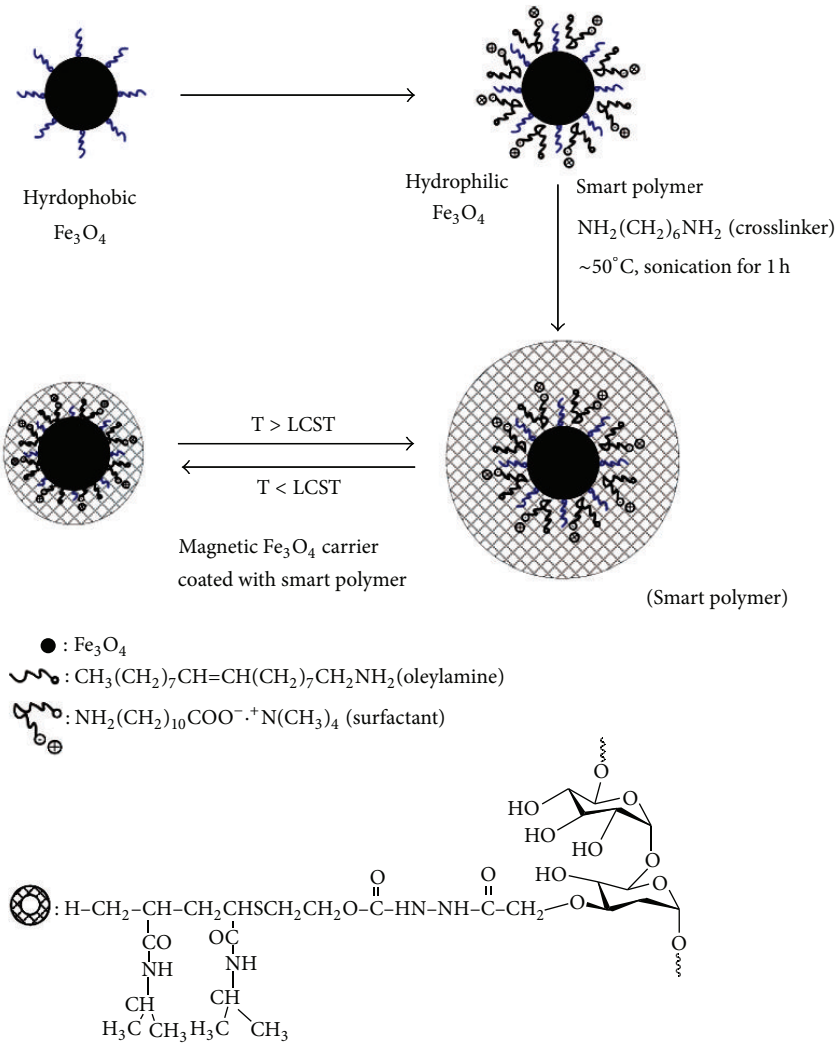

Figure 4: Schematic illustration of the magnetic carrier coated with smart polymer [51].

Lee et al. synthesized poly(aniline)-poly(styrenesulfonate)@Fe_3O_4 core-shell nanoparticles using aqueous solution that contained PSS@Fe_3O_4 and was added to freshly distilled aniline and APS. The yielded PANI-PSS@Fe_3O_4 core-shell nanoparticles are dark-green solids [28]. Liu et al. have synthesized SiO_2@polypyrrole conductive core-shell nanoparticles [29]. In situ polymerization of pyrrole monomers leads to these structures. Through this approach, the core-shell nanoparticles as well as hollow pyrrole nanoparticles are obtained. For hollow nanoparticles the core is etched off by HF. The shell thickness could be controlled by adjusting the monomer concentration and hydrothermal temperature (Figure 16). Through this method large quantities of core-shell conductive and hollow nanoparticles could be obtained via in situ polymerization under hydrothermal conditions.

3. Properties

Controlling the size of the core and thickness of the shell are of paramount significance in tailoring the properties of core-shell nanomaterials. Core-shell structure has attracted much attention as the extra dimension of control over the core NPs. For optimal control of the properties, an ideal sample of core/shell nanoparticles (NPs) should form a stable structure. It has different physical, chemical, and biological properties on the basis of tenability of the composition, surface morphology and structural order of NPs.

3.1. Physical Properties. The core-shell nanostructure and surface functionalization of core-shell nanomaterials have a wide range of advancement of properties. The most important properties like upconversion, electrical conductivity, and dielectric properties have been discussed below.

3.1.1. Upconversion Properties. The upconversion (UC) refers to nonlinear optical processes characterized by the successive absorption of two or more pump photons via the intermediate long-lived energy states followed by the emission of the output radiation at a shorter wavelength than the

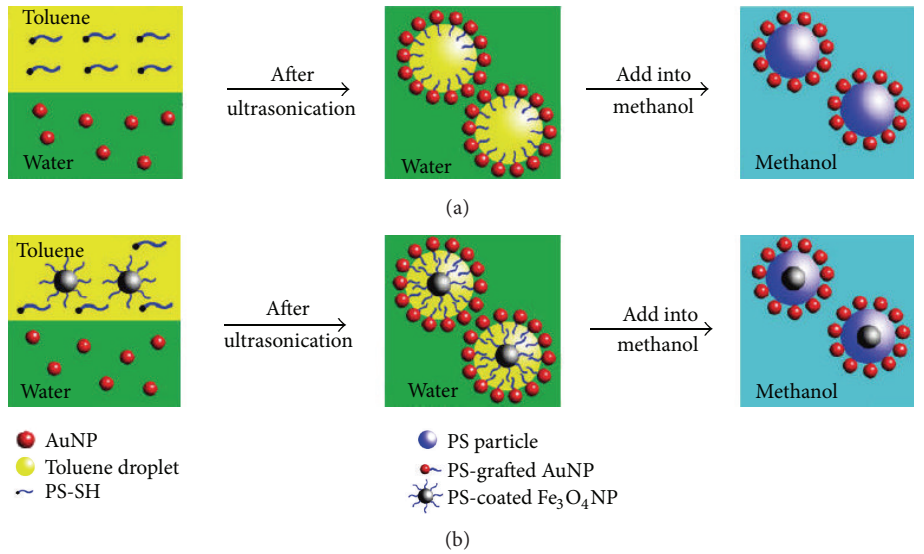

FIGURE 5: Schemes for the preparation of (a) colloidal particles with PS cores and gold nanoparticle (AuNP) coronae and (b) colloidal particles with PS/Fe_3O_4NP core and AuNP coronae [40].

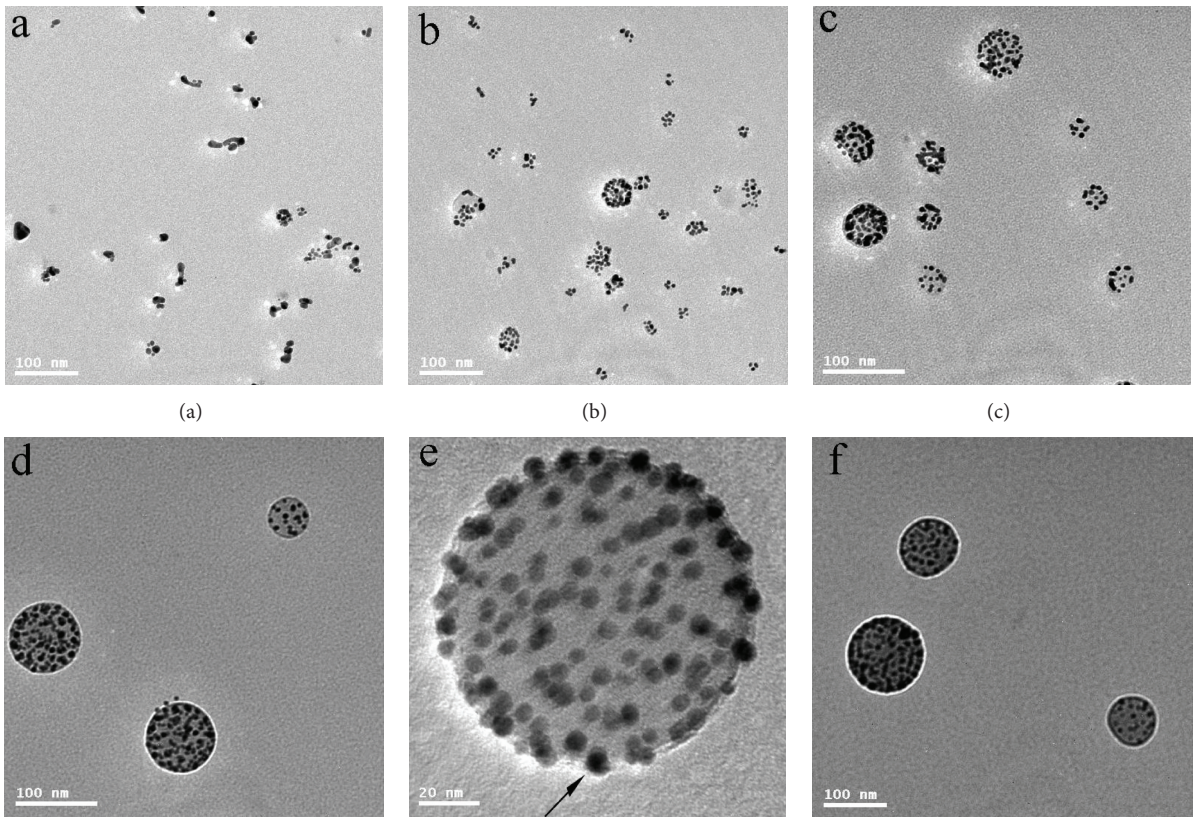

FIGURE 6: TEM images of colloidal particles prepared at different weight ratios of PS-SH to AuNP—(a) 1 : 17, (b) 1 : 4, (c) 1 : 2, and (d) 3 : 1. (e) Magnified TEM image of a colloidal particle showing the details of the structure. (f) TEM image of colloidal particles after changing the solvent from methanol to water [40].

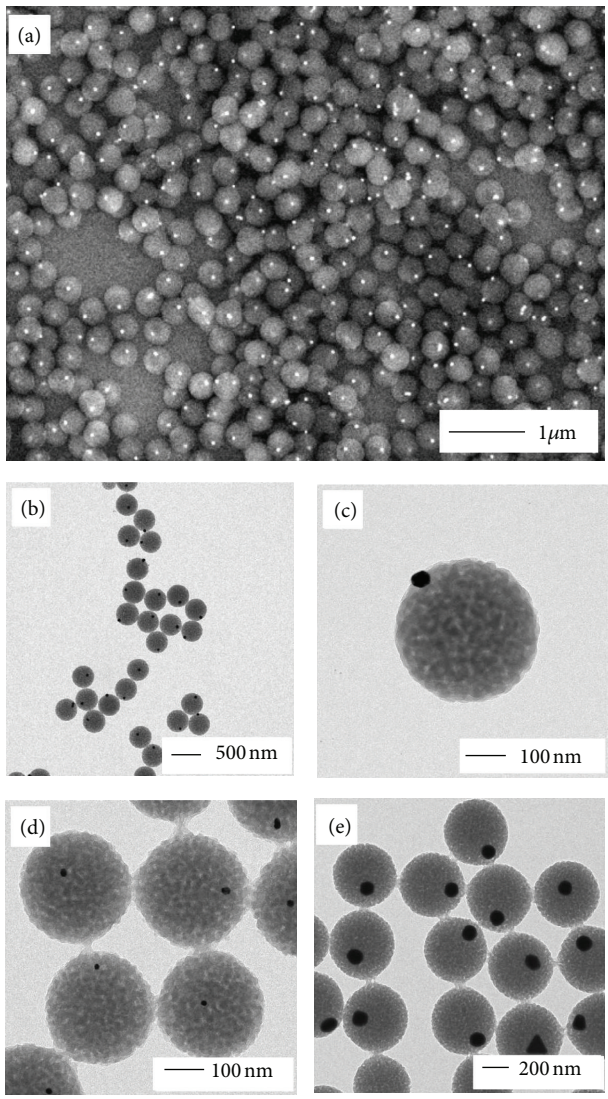

FIGURE 7: (a) SEM and (b–e) TEM images of the eccentric Au-PS particles prepared from Au colloids of different sizes [46].

pump wavelength. Lanthanide ions exhibit unique luminescent properties, including the ability to convert near infrared long-wavelength excitation radiation into shorter visible wavelengths through a process known as photon upconversion. The upconversion intensity of the NPs in aqueous environments was found to be severely quenched when compared to the original NPs in organic solvents. This is due to the high energy vibrational modes of water molecules. This problem could be overcome partially by the synthesis of core-shell NPs which demonstrated improved photophysical properties in water over the original core NPs. Boyer et al. presented a technique for the replacement of oleate with a PEG-phosphate ligand (PEG: poly(ethylene glycol)) as an efficient method for the generation of water-dispersible $NaYF_4$ nanoparticles (NPs) [41]. PEG-phosphate ligands coated upconverting NPs are quite soluble in water and the resulting core-shell structure of $NaYF_4$ is better than core material in imaging cancer cells [41].

Liu et al. synthesized a new type of bifunctional nanocomposites with upconversion nanoparticles and SiO_2 for biomedical applications. The $NaYF_4$:Yb^{3+}, Tm^{3+} was coated with Ru(II) complex doped SiO_2 by combining the upconversion and oxygen sensing properties of individual components (Figure 17) [63]. The upconversion properties and the intensity of the emission and its color from the $NaYF_4$:Yb^{3+}, Tm^{3+} predominantly depends on the concentration of Yb^{3+} and Tm^{3+} in $NaYF_4$ matrix system, the nature of shell, and shell thickness (either it is inorganic or polymer shell), as well as on the liquid dispersion medium (Figures 18 and 19). These bifunctional nanocomposites have potential applications in biochemical and biomedical fields, such as biolabels and optical oxygen sensors, which can measure the oxygen concentrations in biofluids.

Li et al. have worked on the influence of the TGA (Thioglycolic acid) modification on upconversion luminescence of hexagonal-phase $NaYF_4$:Yb^{3+}, Er^{3+} Nanoparticles [56]. The possible conjugation and mechanism of TGA with $NaYF_4$:Yb^{3+}, Er^{3+} nanoparticles is shown in Figure 20 where it is clear that the linking occurred through the–COOH ends. Oleylamine formed a layer on the $NaYF_4$:Yb^{3+}, Er^{3+} nanoparticles and formed a successful stable dispersion.

Fluorescent nanoparticles used for biomedical applications should be small with narrow-size distribution and water-soluble with high luminescent efficiency (Figure 21). First, the Er^{3+} ion is excited from the ground state 4I15/2 level to the excited state 4I11/2 via ET of neighboring Yb^{3+} and Er^{3+}. Subsequent nonradiative relaxations of 4I11/2-4I13/2 populate the 4I13/2 level. In the second-step excitation, the same laser pumps the excited state atoms from the 4I11/2 to the 4F7/2 level via ET, or from the 4I13/2 to 4F9/2 state via phonon-assisted ET. Chen et al. have found that the nY_2O_3/Yb^{3+}/Er^{3+} nanocrystals were enhanced by up to half of the bulk counterpart by tri-doping with Li^+ ions, which can be contrasted to the usually 2 orders of magnitude higher UC radiations of the bulk compared to Li^+-free nanocrystals [64]. Additionally, a remarkable enhancement of emission by three times in ceramic bulk Y_2O_3 suggests the effectiveness of the Li^+ ions for bulk materials, which, however, requires an appropriate technique to dope large concentrations of Li^+ ion into the host lattice for higher enhancement times [64].

3.1.2. Conductivity and Dielectric Properties. Nanoparticles can be easily coated with polymeric shells by electrostatic layer-by-layer assembly of certain polyelectrolytes. The colloidal dispersion stability can be enhanced with polyelectrolyte concentration, contour length of polyelectrolyte chain, and the ionic strength. Core-shell nanocomposites show good conductivity at moderate temperature (283 K to 423 K). According to Yang et al., these properties are prominent for carbon and conductive polymer-(polypyrrol-) based core-shell nanocomposites (C@polypyrrole) (Figure 22) [13]. They also observed the high discharge capacity when they used these composites as electrode materials in supercapacitors in 1.0 M $NaNO_3$ electrolyte solution. The temperature dependence of conductivity of the CB/PPy nanocomposites is represented in Figures 23 and 24. As the temperature increased,

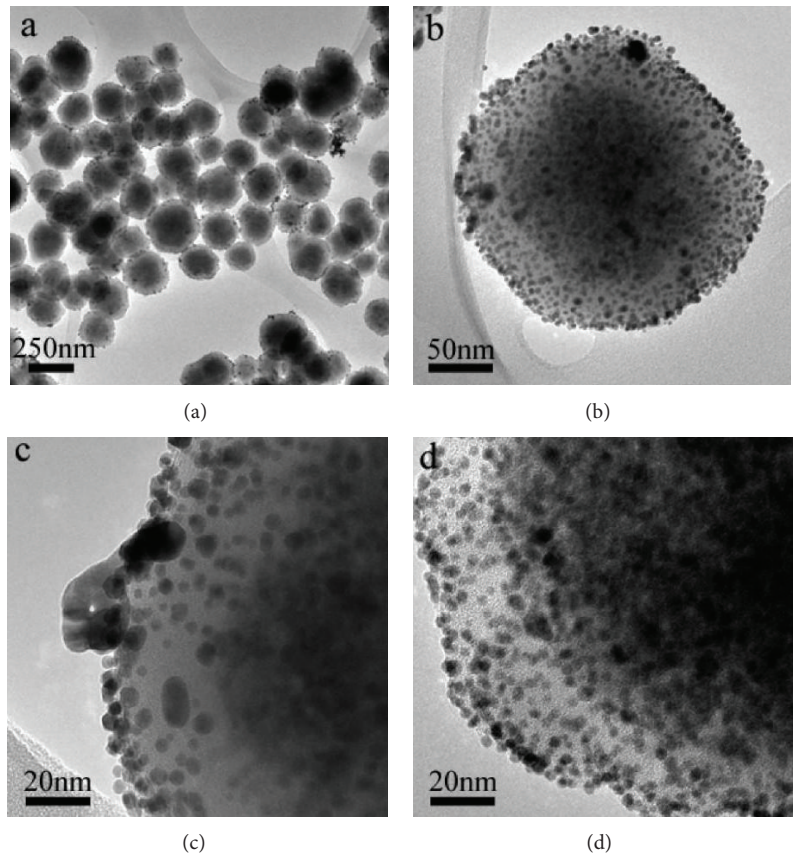

Figure 8: TEM images of the as-prepared Fe_3O_4@SiO_2@Au with core-shell nanocomposite with different magnification (a–c) and the high-magnification TEM image of the as-prepared Fe_3O_4@PANI@Au (d) [47].

the conductivity increased in the range of 283–423 K. The temperature dependence of conductivity indicated that all the samples showed the semiconducting characteristics [13].

Core-shell nanocomposites also show high dielectric constant over a wide range of frequencies. The in situ atom transfer radical polymerization of MMA produces $BaTiO_3$@PMMA core-shell nanoparticles, which shows high dielectric constant over a range of 0.1 Hz to 1 MHz frequencies [14]. The high dielectric loss can be observed only at low frequencies/high temperatures. They also showed low loss of base polymer MMA over a wide range of frequencies. The effective dielectric constant of CSNP hybrids can be tailored by simply changing PMMA shell thickness.

Core-shell nanoparticles possess multiple functional properties. for example, PANI@Fe_3O_4 core-shell nanocomposite exhibits both magnetic and conducting properties [65]. To get PANI@Fe_3O_4 core-shell nanocomposite, the Fe_3O_4 nanoparticles are encapsulated by PANI and dispersed in PANI. In another study, it was found that the more amount of Fe_3O_4 content decreases the crystallinity of the PANI and increases the doping level. As the content of Fe_3O_4 increases, the magnetization of PANI/Fe_3O_4 composite increases simultaneously but conductivity decreases [36]. Li et al. found that the moderate permittivity of the Al_2O_3 layer greatly suppresses the leakage currents and dielectric loss in these nanocomposite materials. Such nanocomposites, with high permittivity, small dielectric loss, and small dependence of permittivity and dielectric loss on temperature, are attractive for physically small capacitors with large energy storage capacities and high rating voltages [65].

3.2. Physicochemical Properties (Magnetic Resonance Imaging, Catalytic Behavior, etc.). Imaging (MRI) experiments with polysiloxane-containing diblock copolymer-coated IONPs showed excellent T(2)-weighted contrast effect from coated IONPs with a transverse relaxivity $r(2) = 98\ 6\,\mathrm{mM}^{-1}\,\mathrm{s}^{-1}$ (at 1.5 T) [57]. Such thin coating layer has little effect on the relaxivity when compared to that of IONPs coated with conventional amphiphilic copolymer. The surface modification of magnetic nanoparticles with thermoresponsive hydroxypropyl cellulose resulting core-shell nanostructure is the excellent candidate for fabricating biocompatible stimuli-responsive magnetic nanoparticles.

Long et al. have synthesized the Pt-Pd core-shell nanoparticles [66]. They studied the comparison of electrocatalytic properties of Pd-Pt bimetallic nanoparticles to confirm their highest catalytic performance. They have noted that catalytic activity of Pt-Pd alloy and core-shell nanoparticles was investigated to develop novel electrocatalysts in direct methanol fuel cells (DMFCs). According to the data analysis, core-shell nanoparticles with the thin nanoshells as monolayers exhibit better nanocatalysts.

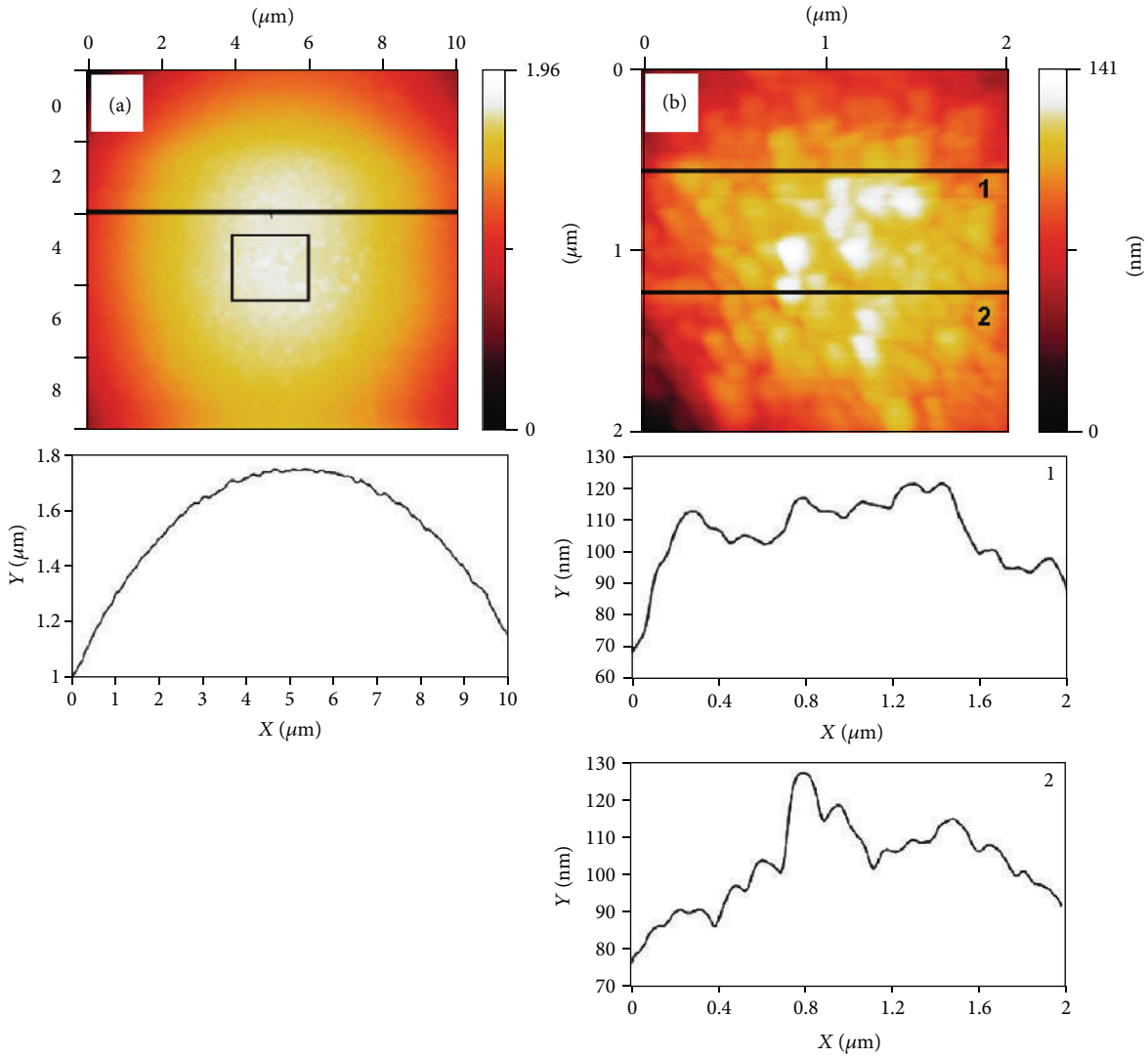

FIGURE 9: AFM surface images (top) of a PS bead covered with AuNPs—(a) single bead (10×10 μm^2), (b) boxed area of bead in (a) (2×2 μm^2) [42].

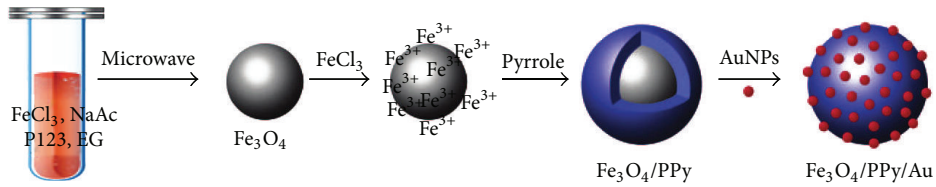

FIGURE 10: Schematic diagram of preparation process of Fe_3O_4/PPy/Au nanocomposites [52].

Alonso et al. also worked on the development of environmentally safe polymer-metal nanocomposite materials containing polymer-stabilized metal nanoparticles (PSMNPs) [67]. These materials can be developed by a functional polymer with immobilized Pd@Co core-shell PSMNPs distributed mainly near the surface of the polymer which makes PSMNPs maximally accessible for reagents in catalytic applications. All PSMNPs nanocomposites were used to check the effective catalytic behaviors in Suzuki cross-coupling reactions between arylboronic acids and aryl halides to produce biphenyls as a reference reaction [67]. The $BaTiO_3$ and ZrO_2 core-shell nanoparticles having variable Al_2O_3 shell thicknesses can be prepared via a layer-by-layer deposition of methylaluminoxane. With increasing or

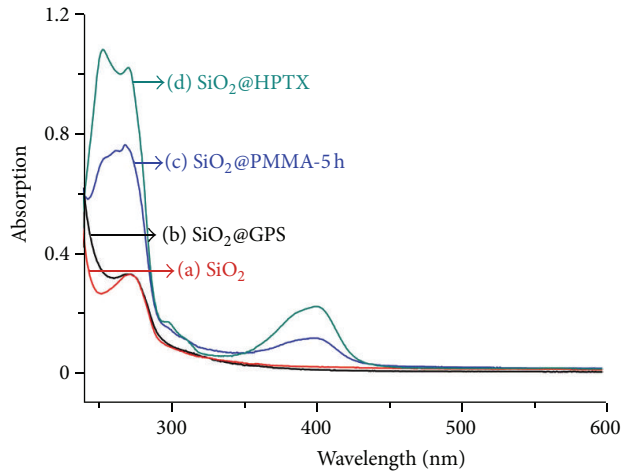

Figure 11: UV-Vis spectra of (a) SiO_2 (raw SPs), (b) SiO_2@GPS, (c) SiO_2@HPTX, and (d) SiO_2@PMMA-5 h in toluene [17].

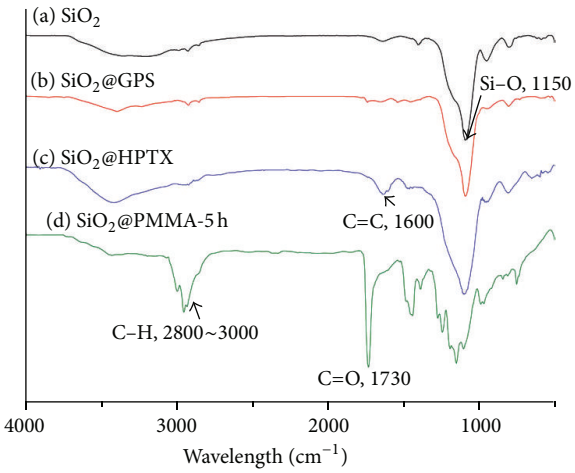

Figure 12: FT-IR spectra of (a) SiO_2 (raw SPs), (b) SiO_2@GPS, (c) SiO_2@HPTX, and (d) SiO_2@PMMA-5 h [17].

decreasing the Al_2O_3 shell thickness, the leakage current and high-field dielectric loss in these core-shell nanocomposites can be tuned [65].

Recently, a few research articles on inorganic-inorganic/polymer-inorganic core-shell nanoparticles have been reported by Guo and coresearchers [68–75]. They found various improved functional properties like dielectric, thermal, magnetic, anticorrosion, and so forth. It was observd that Fe@SiO_2 and Fe@SiO_2/polyurethane nanocomposites have improved thermal stability and antioxidation capability compared to the Fe@FeO and Fe@FeO/polyurethane [69]. Fe@SiO_2/PU can absorbe electromagnetic radiation with high extent. Carbonyl-iron-particles-(CIP-) silica/PU composites are very much potential for anticorrosive behavior than that of the CIP/PU composites [70]. In another work it was found that CIP-silica particles and CIP-silica/PU composites are quite thermally stab and with more enhanced antioxidation capability than that of their counterparts [72].

3.3. Biological Properties

3.3.1. Surface Modification and Biocompatibility Properties. Hydroxypropyl cellulose is a biocompatibility as well as biodegradable polymer. Polysiloxane-containing diblock copolymer-coated IONPs are stable without aggregation or binding to proteins in serum when incubated in cell culture medium containing 10% serum (Figure 25). Furthermore, a much lower level of intracellular uptake by macrophage cells was observed with polysiloxane-containing diblock copolymers-coated IONPs, suggesting the reduction of non-specific cell uptakes and antibiofouling effect [57].

Au nanoparticles of size between 5 and 20 nm coated with densely packed polymer chain showed greater efficiency in cellular uptake [68]. The high grafting densities, surface properties, and size of the hybrid nanoparticles should be the only contributing factors in cellular uptake in epithelial Caco cells. Negatively charged AuNPs can be taken up easily by the cells with greater efficiency than the neutral AuNPs, most probably due to binding with membrane proteins. The positively charged AuNPs increase the uptake efficiency. The oxidation can be catalyzed by the metal@T-CoS-MiP nanocomposites at room temperature in water using air as oxidant. The Au nanocomposite particles show the enhanced catalytic activity for the oxidation of benzyl alcohol [68]. Moreover, it was found that the catalytic activity of the metal nanocomposite can be modulated by the volume transition of microgel particles for the oxidation reaction of benzyl alcohol [68]. Wu et al. studied the influence of the experimental parameters in the formation of silver/polypyrrole core-shell nanoparticles [39]. Core-shell-structured hybrid nanogels (40–80 nm) composed of Ag nanoparticles as core and smart gel of poly (N-isopropylacrylamide-co-acrylic acid) as shell have been synthesized by Wu et al. The pH-induced shrinkage of the nanogel increases the UV-vis absorption intensity and causes blue shift of the surface plasmon bands of the Ag NPs core. The smart nanogel can overcome cellular barriers to enter the intracellular region and light LIP the mouse melanoma $B_{16}F_{10}$ cells, including the nuclear regions. The surface property and concentrations of the hybrid nanogels influence their interactions with cells, resulting in different cell morphology and selective cell staining. The pH-responsive hybrid nanogels exhibit not only a high drug loading capacity but also a pH-controllable drug releasing behavior.

3.3.2. Thermoresponsive Properties. Core-shell structures with thermal responsive poly(N-isopropyl acryl amide) (PANIPAM) as core and gold nanoparticles as shell were synthesized [43]. The fabrication process is easy because there is no need to change or modify the structures of PANIPAM and AuNPs. The Ag@polystyrene core-shell nanoparticles show an increase in the surrounding dielectric constant. Extinction spectra show red shift which is conformation of characteristic plasmon frequency (Figure 26). These particles can be synthesized by hydrogen reduction of silver oxide solution at elevated temperatures in the presence of polystyrene microspheres followed by acetone treatment [43].

Guo et al. synthesized size tunable degradable nanoparticles and they have studied thermal properties of these

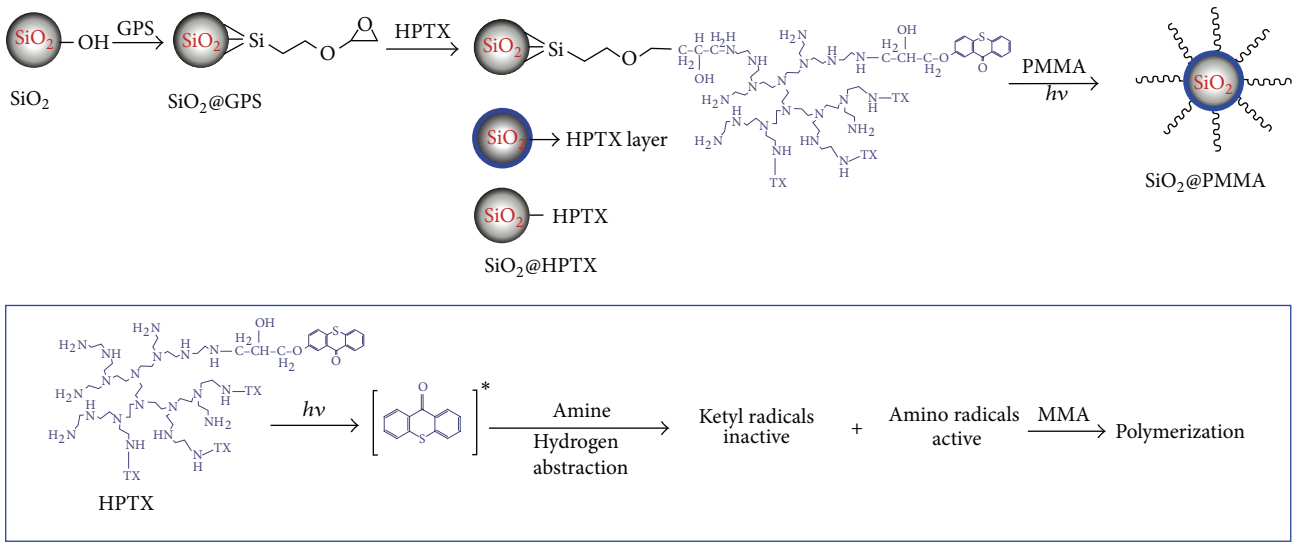

Figure 13: Schematic showing preparation of silica nanostructure and their mechanism [17].

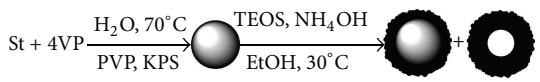

Figure 14: Schematic illustration for the formation of silica-coated latex particles and hollow particles [26].

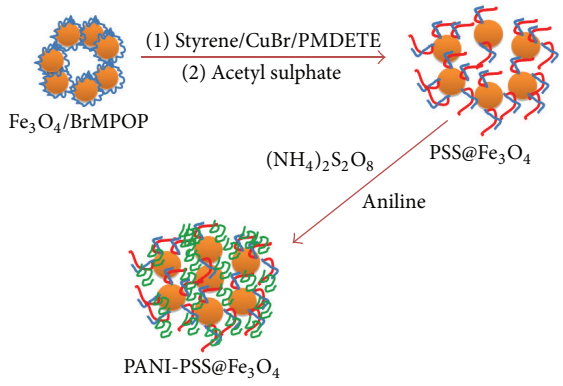

Figure 15: Schematic representation for the synthesis of polyaniline-poly(styrene sulfate)@Fe_3O_4 nanoparticles.

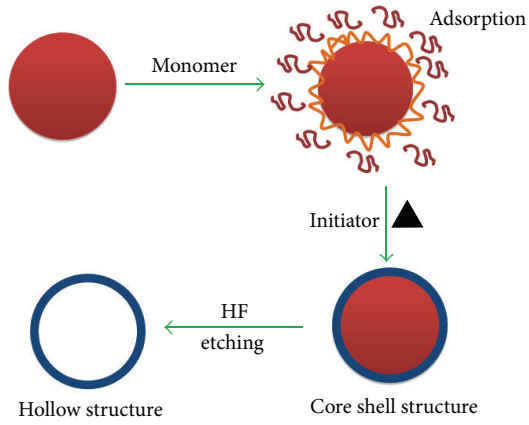

Figure 16: Formation mechanism of SiO_2/polypyrrole conductive core-shell and hollow core nanostructure.

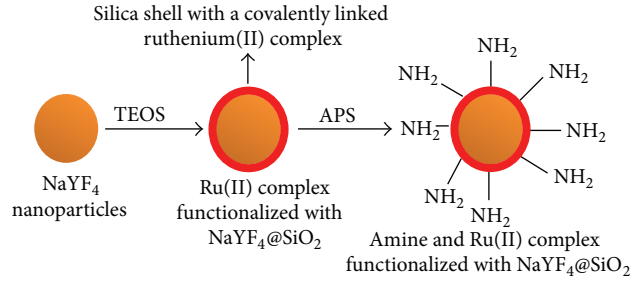

Figure 17: Synthetic scheme for the bifunctional upconversion of oxygen-sensing nanocomposites.

polymers which are also very important for high temperature applications [76]. The TGA thermograms of the triblock copolymers are shown in Figure 27. This thermal degradation behavior of polycaprolactone-emeraldine state aniline pentamer polycaprolactone (PCL-EMAPPCL) copolymers is similar to that of the AD-PCL (aniline dimer polycaprolactone) polymers. In the case of the PCL-EMAP-PCL copolymers, the first obvious weight loss took place in the temperature range between 310°C and 440–460°C, attributed to the decomposition of the less thermally stable PCL segments (Figure 27). They observed that if the temperature is increased from 440 to 460°C and to 620°C, there was a second evident weight loss of about 25–10 wt % of the copolymer, which corresponds to the degradation of the EMAP segment. Thermal degradation occurs at a lower temperature in the case of the AD-PCL polymers, this is indicating that the PCL-EMAP-PCL copolymers have a higher thermal stability.

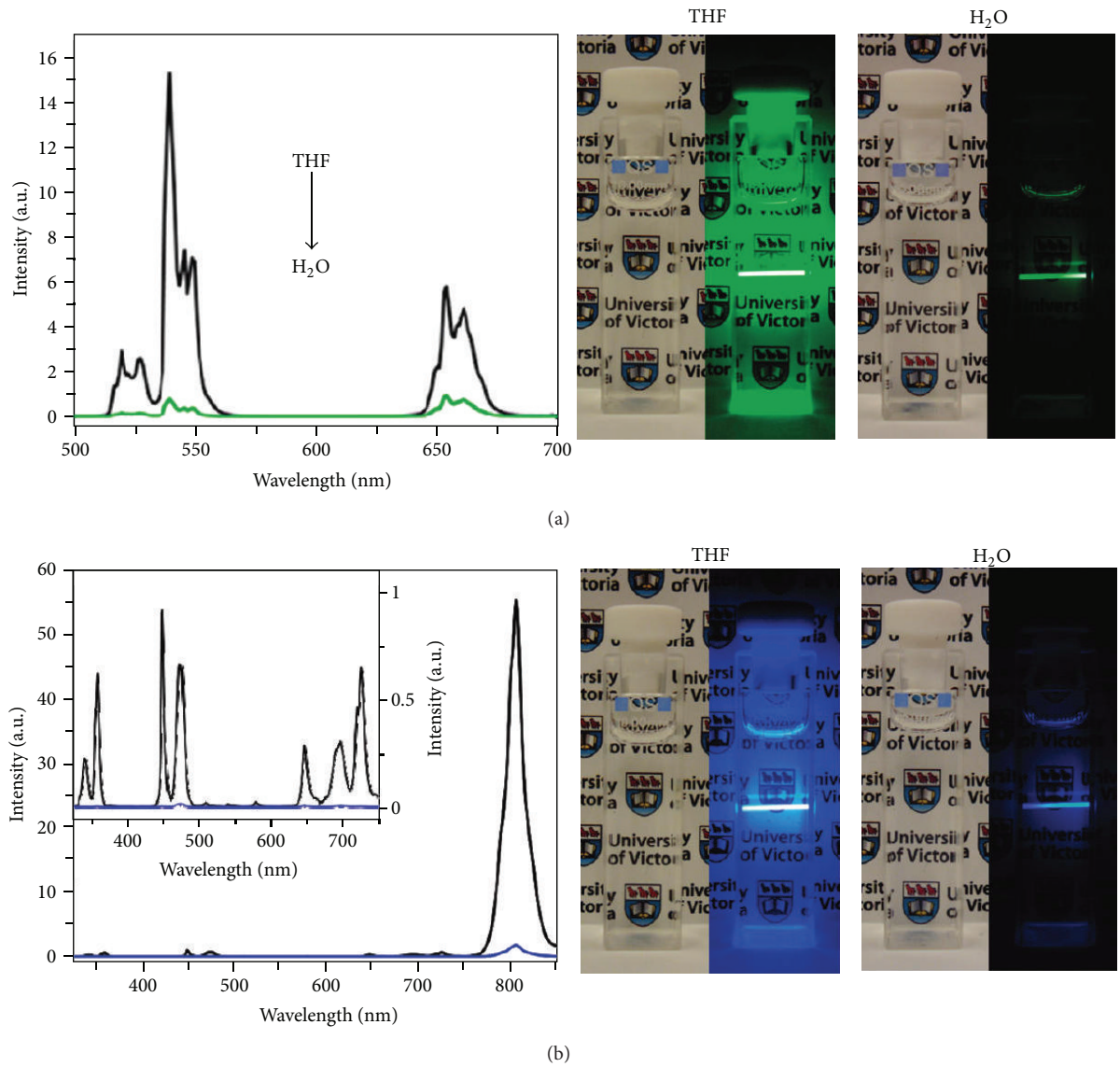

FIGURE 18: Upconversion spectra of original oleate-stabilized NPs in THF and PEG (2000)-phosphate coated NPs in water. (a) $NaYF_4$:Er^{3+} 2 mol %, Yb^{3+} 20 mol% NPs. (b) $NaYF_4$:Tm^{3+} 0.5 mol%, Yb^{3+} 30 mol% [41].

3.3.3. pH Responsive Properties. pH responsive optical properties of core-shell materials have a potential in biomedical applications. Photoluminescence (PL) of the Ag nanocrystals can be tuned in multiple sensitive hybrid microgels. The microgels can be embedded with Ag nanoparticles or Ag@Au bimetallic nanoparticles. The multiple sensitive copolymer microgels of poly(n-isopropylacrylamide-co-acrylic acid-co-acrylamide with polyacrylamide fragments can serve as stabilizing. The photonization of poly(acryl acid) fragments shrinks the microgels resulting in the increment of photoluminescence intensity. Blue shift of the emission maximum of the AG nanoparticles conforms this phenomenon. The surface modification of small Ag nanoparticles with Au nanoclusters reduces the pH sensitivity of PL property changes but dramatically enhanced the PL signals in the near-infrared regime of the hybrid microgels [44]. Micrometer-sized silica sol stabilized polystyrene nanoparticles and submicrometer sized polystyrene nanoparticles were synthesized by Schmid et al. Initiator of polymerization has effect on the size of core-shell nanoparticles. When nonionic AIBN initiator is used, micrometer-sized polystyrene@silica sol core-shell nanoparticles are obtained. When this cationic initiator is used, the submicrometer and nanometer-sized polystyrene silica nanocomposites were obtained. Reduction of initial silica concentration results in the increase in the overall latex diameter. By calcinating these core-shell nanoparticles we can have hollow silica nanocapsules [31].

Yang et al. employed the pH sensitivity property of polymer microspheres/micelles with DOX (doxorubicine hydrochloride) as a model drug for cancer treatment [77]. The loading behavior of DOX in hollow P(MBAAm-co-MAA) microspheres depends on the pH of the medium. For

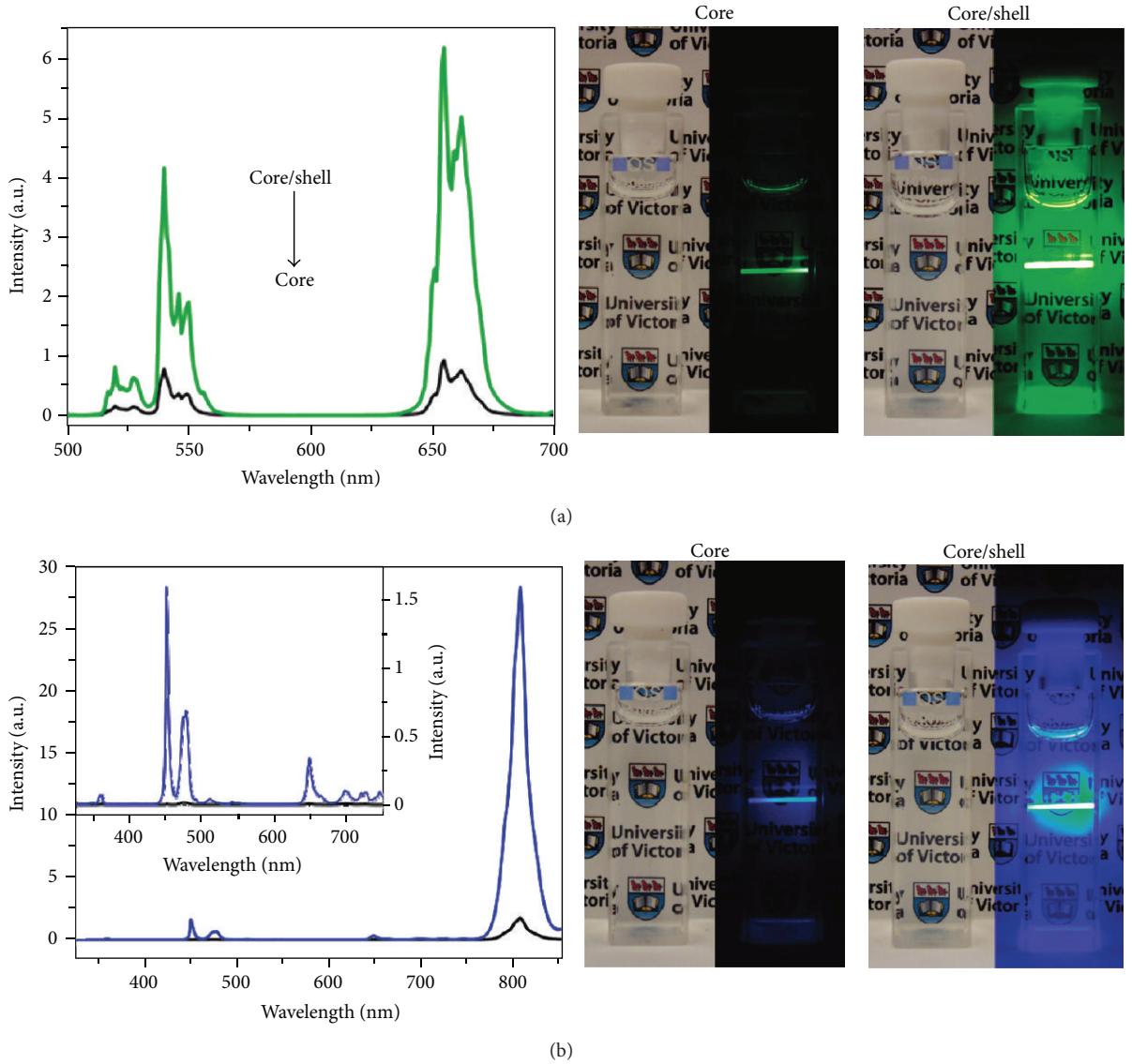

Figure 19: Upconversion spectra of PEG(2000) phosphate-coated NPs in water. (a) $NaYF_4$:Er^{3+} 2 mol %, Yb^{3+} 20 mol%, and NaYF4:Er^{3+} 2 mol %, Yb^{3+} 20 mol%/$NaYF_4$ core-shell NPs. (b) $NaYF_4$:Tm^{3+} 0.5 mol %, Yb^{3+} 30 mol%, and NaYF4:Tm^{3+} 0.5 mol%, Yb^{3+} 30 mol%/$NaYF_4$ core-shell NPs. All samples dispersed as 1 wt % colloids in water [41].

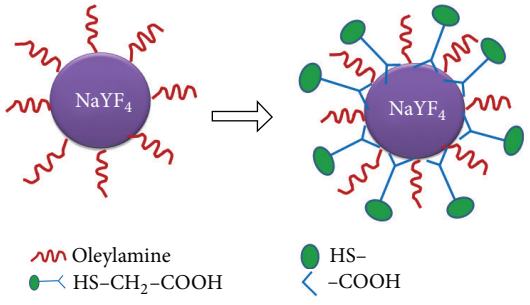

Figure 20: Scheme of surface modification of $NaYF_4$ nanoparticles with TGA (thioglycolic acid).

example, the loading capacity of DOX on hollow P(MBAAm-co-MAA) microspheres was 40 mg/mg at pH of 1, 321 mg/mg, at pH of 7, and 236 mg/mg at pH of 10, respectively. Therefore, the pH level has significant effects on the loading capacity of the DOX in hollow P (MBAAm-co-MAA) microspheres and is a controlling factor.

3.3.4. Surface Functionalization. Surface functionalization plays an important role in achieving the core-shell nanostructures. A study has been done in last few decades and proposed that in the synthesis of polystyrene@ZnO core-shell nanostructures, the interaction between the ZnO nanoparticles and beta-diketone groups present on the surface of the polystyrene particles leads to core-shell nanocomposite structures. In core-shell nanocomposites synthesis, the selection of suitable polymerization initiator decides the efficiency of aggregation of shell on the core. The synthesis of colloidal poly(2-vinylpyridine)-silica nanocomposite particles suitable

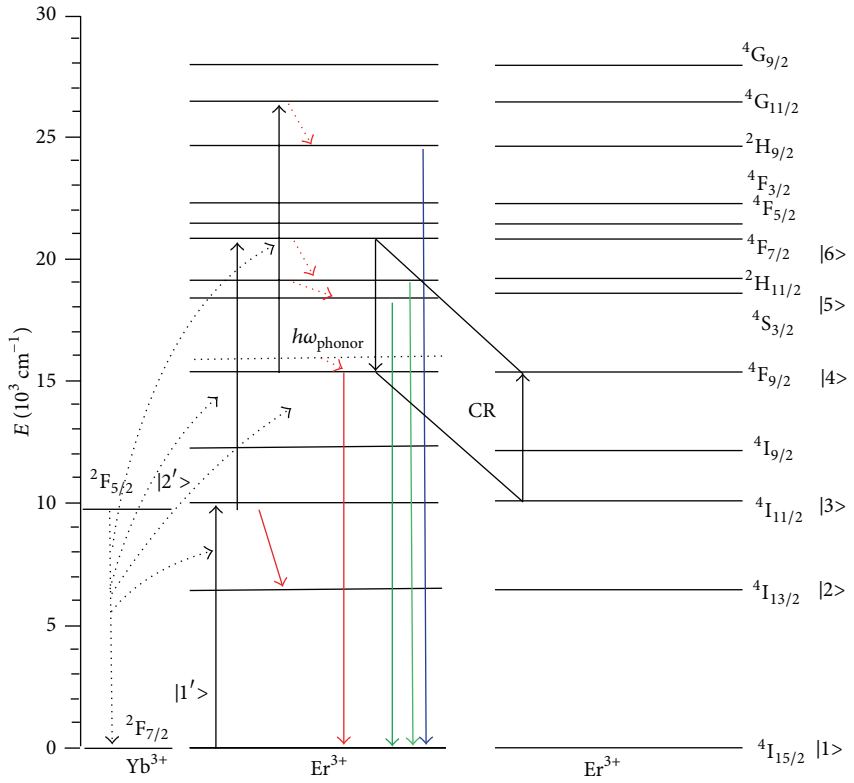

Figure 21: Upconversion population processes in the Yb3+, Er3+ codoped system under 980 nm laser-diode excitation [56].

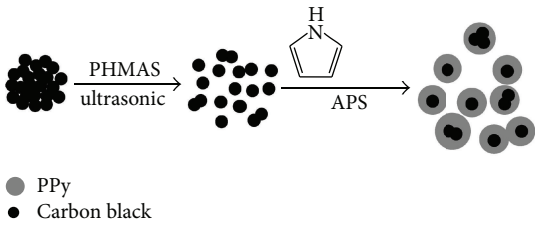

Figure 22: Schematic illustration of the synthesis process of the core-shell CB/Ppy nanocomposite [13].

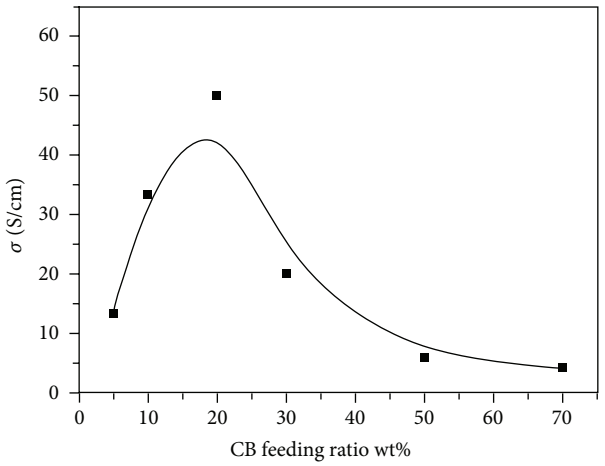

Figure 23: Conductivities of the CB/PPy nanocomposites at room temperature [13].

cationic azo initiator leads to a very high silica aggregation efficiencies (88%–99%) [32]. These nanoparticles, nanostructures and nanocomposites were synthesized using emulsion polymerization. In this the core material can be replaced with some materials like styrene, methacrylic comonomers to produce copolymer-silica core-shell nanocomposites [32]. The composite core-shell nanoparticles give improved properties than the individual nanoparticles. The ultrasonic irradiation synthesis of collagen-grafted PMMA/Ag@TiO_2 composite shows lower infrared emissivity value in the range from 8 to 14 μm than that of pure collagen or grafted collagen (Table 2) [34]. This is the result of strong interfacial synergism forces inside the composite. The thickness of the TiO_2 shell is varied with concentration of Ti precursor. The Ag core diameter produced is around 50 nm [34].

4. Applications

Synthetic polymeric core-shell nanomaterials can be used in medical fields like disposable supply, prosthetic materials, dental materials, implants, dressings, extracorporeal devices, encapsulants, polymeric drug delivery systems, tissue engineered products, and orthodoses as that of metal and ceramics substituents. The core-shell nanoparticles have

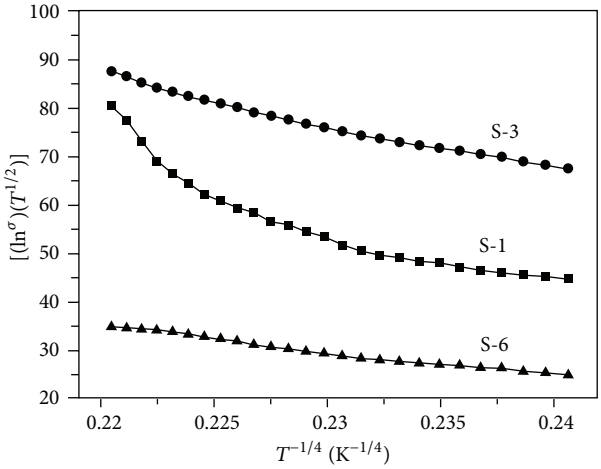

Figure 24: Temperature dependence on conductivity of the CB/PPy nanocomposites based on the VRH model [13].

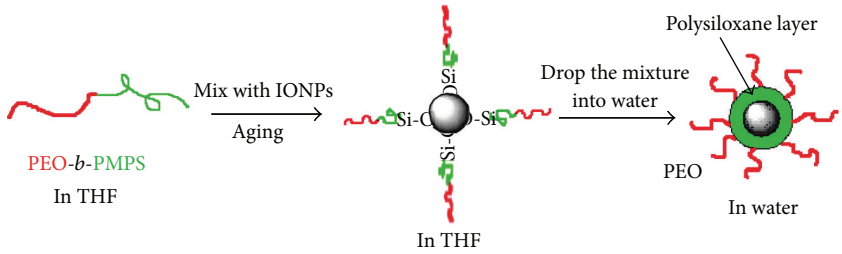

Figure 25: Synthetic pathway for formation of the poly(ethylene oxide)-based macromolecular chain transfer agent [57].

shown a wide range of new applications in the fields of chemistry, bioscience, and material sciences because of their improved physical and chemical properties over their single-component counterpart. Core-shell nanomaterials play important roles in developing biological and medical applications. Proper core-shell materials can provide biocompatibility, safety, and surface functionalization that is required for specific in vitro and in vivo applications.

4.1. Drug Delivery. Buxton and Nigel studied the drug delivery efficiency of polymer core-shell nanoparticles using computer simulations [78]. In particular, they investigated the effects of shell swelling on drug release rates. Polymer core-shell nanoparticles are attractive drug-delivery systems because the drug can be encapsulated inside the core, while the shell properties can be assigned to optimize drug-delivery needs. An elegant approach to such particles is to use polymer gels, which have swelling properties that depend upon conditions such as pH. In this way swelling of the shell, and the drug release, can be targeted to occur at the desired location. Furthermore, they studied the thermodynamic feasibility and investigated both the physical and chemical barriers to drug release from the core shell. Through a combination of structural and fluid simulations, they are able to explain the physics behind polymer core-shell nanoparticles to use it in drug delivery applications [78].

Systems with no enthalpic interactions (Figures 28(a) and 28(b)) are compared with systems which penalize with both drug diffusion out of and bulk fluid into the polymer core. Cross-linked sites are depicted as red (core) and blue (shell) spheres, and the drug molecules are depicted as red mist. Both physical structure and enthalpic interactions play an important role in releasing of the drug from the core-shell nanoparticles. In particular, the amount of drug that has been diffused out of the core-shell particles appears to be larger for the open particle (Figure 28(a)) than for the closed particle (Figure 28(b)) [78]. Poly(amidoamine)(PAMAM)-poly(2-(N,N-diethylamino)ethyl methacrylate)(pDEA)-ethoxy-poly(ethylene glycol)2000 (mPEG) is also a promising nanocarrier for the delivery of anticancer drugs [79]. The pH sensitive and thermosensitive biocompatible polymer core-shell nanoparticles are also a potential for drug delivery and cancer therapy [43, 77].

4.2. Biomedical Application and Drug Carrier. Core-shell nanoparticles play an important role in biomedical applications. The core-shell nanoparticles can be used as drug carriers with sustained release. The drug uptake and release profile can be altered by changing the structuring morphology of core and shell materials. In surfactant-free self-assembled iron nanoparticles (SAIO)@SiO_2 core-shell nanocrystals, the hydrophobic drug molecules can be encapsulated within the SAIO-PVA (surfactant-free self-assembled iron nanoparticles-polyvinyl alcohol) core and then further covered with a thin shell of SiO_2. The structure of the core can

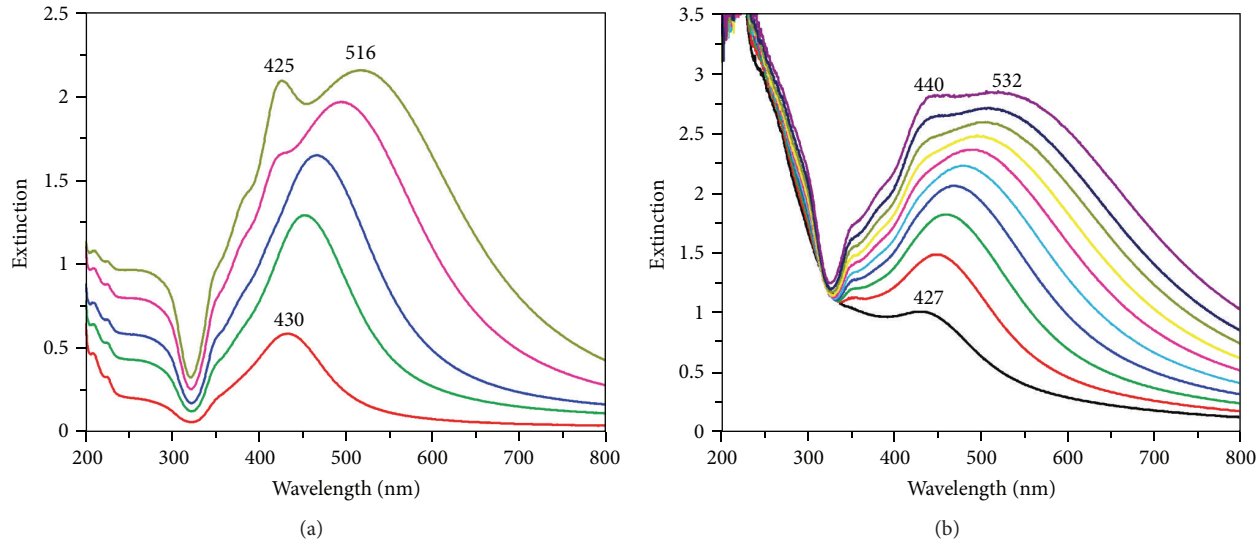

Figure 26: Extinction spectra of AgNPs as they grew in the absence (a) and presence (b) of ~200 nm PS microspheres [43].

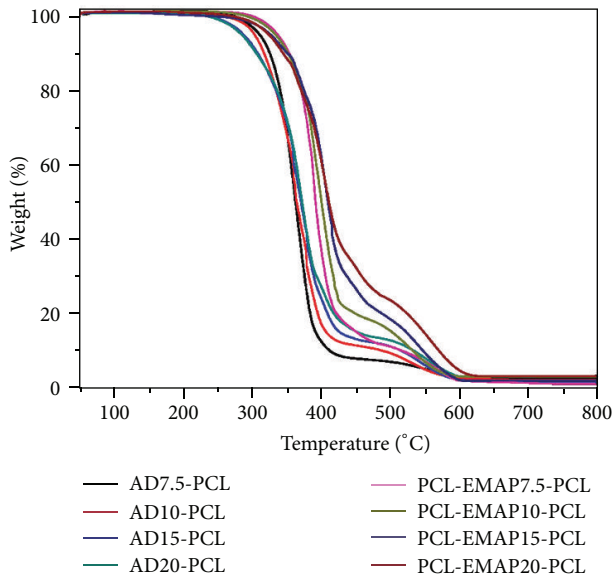

Figure 27: Thermal stability of AD-PCL and PCL-EMAP-PCL copolymers [76].

be distinguished when an external magnetic stimuli is applied resulting in burst release of the drug. After removing external magnetic stimuli drug profiles showed linear and controlled releases. These core-shell nanocrystals also showed high uptake efficiency from the HeLa cancer cells [23].

Fe_3O_4/Polypyrrole/Au nanocomposites with core/shell/shell structure were synthesized by Zhang et al. [52]. These core-shell nanocomposites show magnetism in addition to being easily controllable by an external magnetic field. They also show good conductivity and excellent electrochemical and catalytic properties of PP and Au nanoparticles. Additionally, these nanocomposites showed excellent electrocatalytic activities to biospecies such as ascorbic acid [52]. Some core-shell nanocomposites of PANI and Fe_3O_4 show improved conductivity than that of their individual particles and they can also exhibit multifunctional properties. Fe_3O_4/PANI core-shell nanocomposites showed higher conductivity ($6.4–9.2 \times 10^{-2}$ S/cm) than that of pure PANI (3.7×10^{-3} S/cm). These particles also show superparamagnetism behavior. The method for the preparation of Fe_3O_4/PANI core-shell nanocomposites provides new strategy for the synthesis of multifunctional core-shell nanocomposites (i.e., conducting polymers and metal nanoparticles) [80].

Biocompatible polysiloxane-containing amphiphilic diblock copolymer, poly(ethylene oxide)-block-poly (gamma-methacryloxy propyl trimethoxysilane) (PEO-b-P gamma MPS), can be used for coating and stabilizing nanoparticles for biomedical applications [65]. Human lung cancer cells (H1299) can be imaged by biocompatible nanocomposites. Biocompatible green luminescent monodisperse Ag@pheno formaldehyde resin core-shell nanocomposites were used by Guo et al. [48]. These core-shell nanoparticles are used for in vivo bioimaging by embedding them into the human body. Fluorescent molecules labelled single-molecular core-shell nanospheres of hyperbranched conjugated polyelectrolyte can be used for cell imaging [54].

4.3. Molecular Bioimaging. Molecular bioimaging is one of the most powerful techniques of noninvasive imaging methods utilized in medical sciences, and it is based on the relaxation of protons in tissues. Upon accumulation in tissues, SIONPs enhance proton relaxation of specific tissues compared with that in surrounding tissues, serving as an MR contrast agent [81]. The iron oxide nanoparticles allow the nanocarriers to be used as agents for magnetic resonance imaging (MRI), magnetic targeting with the assistance of external magnetic field gradients and hyperthermia treatment in an alternating magnetic field [14, 15]. The core-shell has tunable magnetic and biocompatible properties and it can

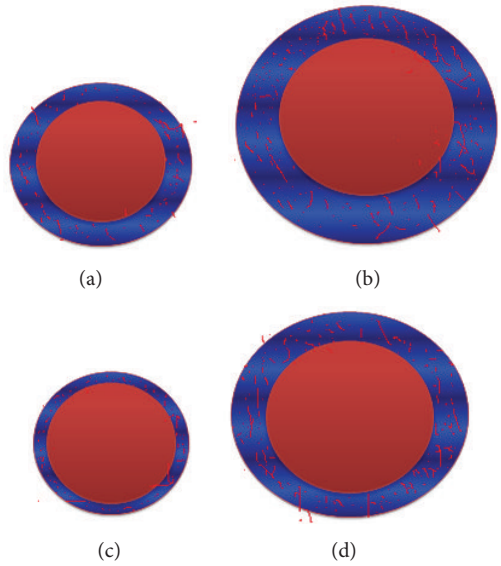

Figure 28: Schematically the drug diffusion mechanism from the core-shell nanoparticles is shown. The drug diffused out of closed (a and c) and opened (b and d) nanoparticles. Systems with no enthalpic interactions (a and b) are compared with systems which penalise both drug diffusion out of and bulk fluid into the polymer core (c and d).

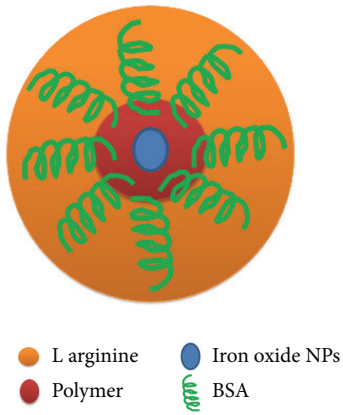

Figure 29: Schematic representation of the iron oxide core-shell nanoparticles.

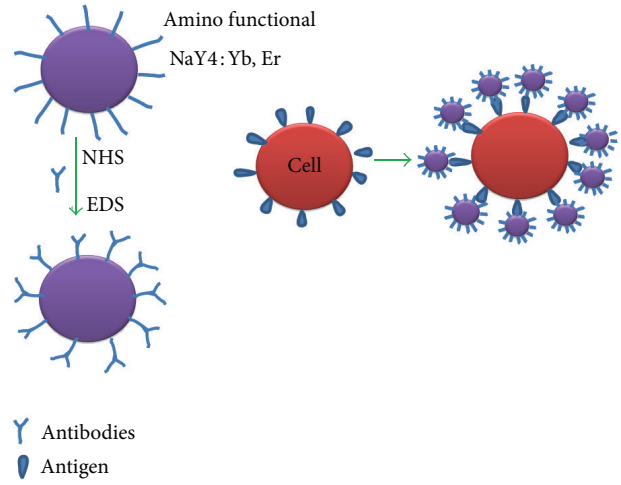

Figure 30: Schematic representation of immunolabeling of HeLa cancer cells with UCN, antigen, and antibodies.

be used in various types of bioimaging technique (e.g., CT scan, MRI, etc.). Several types of polymer DDS have been exploited, including polymer prodrugs [73], micelles, and vesicles based on amphiphilic and double-block copolymers [82, 83], dendrimers [84], and hydrophobic polyester-based nanoparticulates [85] molecular bioimaging. Yathindranath et al. synthesized surface-modified iron oxide core-shell nanocomposites with different biocompatible polymers along with an excipient during freeze-drying. They observed that bovine serum albumin (BSA) was physically adsorbed onto the surface of iron oxide nanoparticles along with excipient during the freeze-drying. The BSA attached with iron oxide nanoparticles when applied the magnetic field of an MRI instruments was observed in vitro due to the mass transport [86]. The designed polymer core-shell materials, as shown in Figure 29, are used for bioimaging under the magnetic field.

The schematic of the IO CS-NPs is represented in Figure 29. PEG is chosen as coating, since, it is a neutral, hydrophilic polyether. PEG is known to form stable protein conjugates. PEG is also nonimmunogenic and nonantigenic with a long in vivo circulation lifetime [86].

Achieving the dual functions of MRI and magnetic targeting, a strategy was developed to synthesize CMD (carboxymethyldextran) coated, iron oxide-based core-shell magnetic nanoparticles with controlled sizes. Characterization demonstrated that the nanoparticles thus synthesized possessed a shell-core structure consisting of a thin polymer shell coating on a self-assembled magnetic core made of

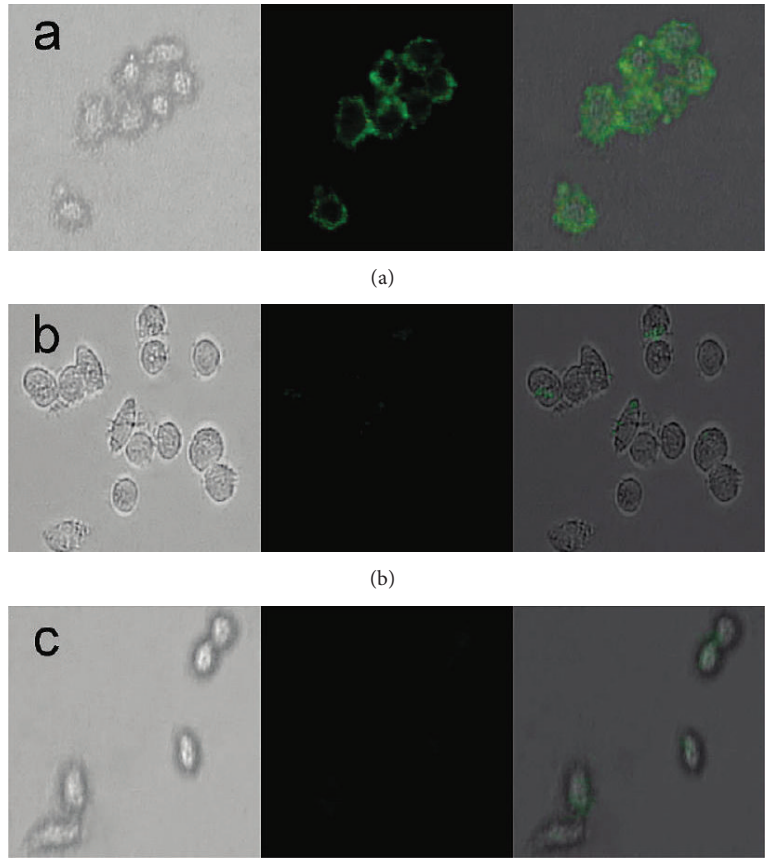

Figure 31: Fluorescence imaging of HeLa cells after incubated with rabbit anti-CEA8 Ab-conjugated UCNPs (a), amino-modified NPs without linking any antibody (b), and rabbit anti-goat Ab-conjugated UCNPs (c) for 1 h. Left rows are images in bright field; the middle rows are fluorescent images in dark field; and right rows are overlays of the left and middle rows [88].

agglomeration of superparamagnetic, monocrystalline iron oxide nanoparticles (MION) [87].

4.4. PhotoSensitive Applications. In some core-shell hybrid nanoparticles, the photochromic properties can be changed by changing the precursor ratios synthesis. In spiropyran@silica core-shell nanoparticles, the chemical nature and porosity can be changed by changing the precursor ratio. Depending upon the content of the MTEOS the optical response can be tuned from reverse to direct. The nanoporous shell in which silylated spiropyran-derived chromophore is grafted [19]. The core-shell structure can be modified by the fluorescence molecules. By changing the content of ZnO particles into polymer-coated ZnO, the strong blue fluorescence with quantum yield more than 80% is achieved. In this, the different fluorescence mechanism is suggested for pure ZnO. The surface of the ZnO was modified by methacrylic group to initiate the polymerization by reacting with liquid monomers. The core-shell microgels consist of a polystyrene core and a network made of poly(N-isopropylacrylamide) (PNIPA) cross-linked by N, N′-methylenebisacrylamide which are used as "nanoreactors" for the immobilization of metal nanoparticles like those in [89]. Core-shell materials can be used as plasticizers to improve toughness and stiffness of the matrix material [49]. PMMA(PBA) core-shell nanoparticles can be used to improve the degree of dispersion and compatibility of the phosphors like SrAl(2)O(4) $Eu^{(2+)}$, $Dy^{(3+)}$ in the PVC matrix. The results for PVC plastics characterized by SEM show that the interfacial adhesion was enhanced with filling the polymer/phosphor composite particles, and the compatibility of phosphor with PVC matrix was improved by coating with PMMA(PBA). The luminescent PVC plastics filled with PMMA(PBA)/phosphor composite particles show improved mechanical properties and higher phosphorescence when the filling content was more than 3 phr compared with the unmodified phosphor [90].

4.5. Immunolabeling and Imaging of HeLa Cells. Wang et al. worked on upconversion fluorescent nanoparticles [88]. Upconversion nanoparticles can convert a longer wavelength radiation (e.g., near-infrared, NIR light) into shorter wavelength fluorescence (e.g., visible light) and thus have emerged as a new class of fluorescent probes for biomedical imaging. The cells exhibited bright green UC fluorescence, confirming the attachment of the antibody-UCNP conjugates on the surface of cells (Figure 30). This fact indicates that the UCNPs

with good biocompatibility recognized the targets on the cell membrane due to the antibody conjugation, and the UC fluorescence was strong enough for the cell imaging. The shape and position of the cells in bright field and dark field overlapped very well, showing good specific interactions between the UCNPs and the cells. As drawn in Figure 31, amino-modified $NaYF_4$:Yb, Er UCNPs were first cross-linked with the rabbit anti-CEA8 antibody (Ab), which involves a simple condensation reaction between carboxyl groups of antibody and amino groups on the surfaces of the NPs by the aid of NHS and EDC [88]. Surface modification of gold nanorods using bovine serum albumin (BSA) and polyethylenimine (PEI) enabled cellular imaging using light scattering from the NRs [91]. Polymeric liposomes-coated superparamagnetic iron oxide nanoparticles (SPIONs) show better T(2)-weighted images than uncoated nanoparticles [92]. In conclusion, polymer-based UCN core-shell nanoparticles have better prospect as fluoresce probe marker and light sensitive materials for therapeutic application.

4.6. Cancer/Tumor Treatment. Hyperthermia therapy with SIONPs (size-dependent iron oxide nanoparticles) involves a local increase in temperature (up to 45°C) when external magnetic field is applied on SIONPs. Such a temperature increase can be lethal for temperature-sensitive cells, such as cancer cells. Recent studies using calorimetry shows that the heating rate depends on the particle size of the SIONPs, consistent with theoretical predictions. This result suggests that the SIONPs should be designed to have optimal particle size with narrow-size distribution for enhanced hyperthermia therapy [93].

5. Conclusions and Future Aspects

There are different types of core-shell structures. Based on these metal, nonmetal, and polymers core-shell nanostructures, they can be categorized in many. The core-shell structures maintain their integrity when redispersed in water. The core-shell structures represent a new class of metal-polymer composite materials that can be used for photonic and biomedical applications exploiting optical properties.

The primary focus in research and technology develop significant contributions to the modern civilization through the invention of the new types of core-shell nanostructure. The core-shell nanostructure, pure polymer nanoparticles, and core-shell hybrid nanoparticles with functional properties can be utilized for the various types of applications and molecular materials, which can gradually "disappear," that is, degrade to harmless small molecules and fragments, after successful performance of their task in various biomedical and environmental applications. Core-shell and hybrid core-shell nanoparticles will be playing a key role in the design of the medical devices, especially in drug delivery, tissue engineering, and plastic surgery. Researchers are involved more to use the core-shell nanoparticles as structure materials to use them in drug delivery, drug targeting, bioimagination, sensor applications, dielectric properties-based devices, and so forth. These materials show good future aspects in all the fields of biotechnology such as cancer therapy, sustained and targeted drug delivery. Recently, much attention has been focused on metal nanoparticles such as gold, platinum, and palladium because their properties may markedly differ from the ones of the respective bulk metals. Authors of this paper predict that the polymer-based core-shell functional nanoparticles have potential future compared to the inorganic-inorganic nanoparticles in biomedical applications because, polymers are very soft materials, a great number of polymer particles are biocompatible, as well as biodegradable. Polymer shell is easy to modify chemically to develop the functional properties specially for the site-specific target-oriented delivery. On the degradation of the polymers, they only produce C-and-N based components in the living system which is less toxic compared to the inorganic complex formed in the biochemical reactions.

Authors Contribution

K. S. Kumar and V. B. Kumar contributed equally to this paper.

References

[1] C. Burda, X. Chen, R. Narayanan, and M. A. El-Sayed, "Chemistry and properties of nanocrystals of different shapes," *Chemical Reviews*, vol. 105, pp. 1025–1102, 2005.

[2] P. V. Kamat, "Photophysical, photochemical and photocatalytic aspects of metal nanoparticles," *Journal of Physical Chemistry B*, vol. 106, no. 32, pp. 7729–7744, 2002.

[3] F. Frederix, J. M. Friedt, K. H. Choi et al., "Biosensing based on light absorption of nanoscaled gold and silver particles," *Analytical Chemistry*, vol. 75, no. 24, pp. 6894–6900, 2003.

[4] S. Praharaj, S. Nath, S. K. Ghosh, S. Kundu, and T. Pal, "Immobilization and recovery of Au nanoparticles from anion exchange resin: resin-bound nanoparticle matrix as a catalyst for the reduction of 4-nitrophenol," *Langmuir*, vol. 20, no. 23, pp. 9889–9892, 2004.

[5] C. T. Campbell, S. C. Parker, and D. E. Starr, "The effect of size-dependent nanoparticle energetics on catalyst sintering," *Science*, vol. 298, no. 5594, pp. 811–814, 2002.

[6] T. A. Skotheim, *Handbook of Conducting Polymers*, vol. 1, 1986.

[7] M. G. Kanatzidis, "Polymeric electrical conductors," *Chemical and Engineering News*, vol. 1990, pp. 36–54, 1990.

[8] P. Andersson, R. Forchheimer, P. Tehrani, and M. Berggren, "Printable all-organic electrochromic active-matrix displays," *Advanced Functional Materials*, vol. 17, no. 16, pp. 3074–3082, 2007.

[9] Y. Liu and T. Cui, "Polymeric integrated AC follower circuit with a JFET as an active device," *Solid-State Electronics*, vol. 49, no. 3, pp. 445–448, 2005.

[10] S. K. Lee, J. M. Cho, Y. Goo et al., "Synthesis and characterization of a thiazolo[5,4-d]thiazole-based copolymer for high performance polymer solar cells," *Chemical Communications*, vol. 47, no. 6, pp. 1791–1793, 2011.

[11] L. L. Chua, J. Zaumseil, J. F. Chang et al., "General observation of n-type field-effect behaviour in organic semiconductors," *Nature*, vol. 434, no. 7030, pp. 194–199, 2005.

[12] H. N. Tsao, D. Cho, J. W. Andreasen et al., "The influence of morphology on high-performance polymer field-effect transistors," *Advanced Materials*, vol. 21, no. 2, pp. 209–212, 2009.

[13] C. Yang, P. Liu, and W. Tingmei, "Well-defined core-shell carbon black/polypyrrolenanocomposites for electrochemical energy storage," *ACS Applied Materials & Interfaces*, vol. 3, pp. 1109–1114, 2011.

[14] L. Xie, X. Huang, C. Wu, and P. Jiang, "Core-shell structured poly(methyl methacrylate)/$BaTiO_3$ nanocomposites prepared by in situ atom transfer radical polymerization: a route to high dielectric constant materials with the inherent low loss of the base polymer," *Journal of Materials Chemistry*, vol. 21, no. 16, pp. 5897–5906, 2011.

[15] Q. Rong, A. Zhu, and T. Zhong, "Poly (styrene-n-butyl acrylate-methyl methacrylate)/silica nanocomposites prepared by emulsion polymerization," *Journal of Applied Polymer Science*, vol. 120, no. 6, pp. 3654–3661, 2011.

[16] V. V. Annenkov, E. N. Danilovtseva, V. A. Pal'shin et al., "Poly(vinyl amine)-silica composite nanoparticles: models of the silicic acid cytoplasmic pool and as a silica precursor for composite materials formation," *Biomacromolecules*, vol. 12, no. 5, pp. 1772–1780, 2011.

[17] F. Chen, X. Jiang, R. Liu, and J. Yin, "Well-defined PMMA brush on silica particles fabricated by surface-initiated photopolymerization (SIPP)," *ACS Applied Materials and Interfaces*, vol. 2, no. 4, pp. 1031–1037, 2010.

[18] P. Reiss, E. Couderc, J. De Girolamo, and A. Pron, "Conjugated polymers/semiconductor nanocrystals hybrid materials—Preparation, electrical transport properties and applications," *Nanoscale*, vol. 3, no. 2, pp. 446–489, 2011.

[19] J. Allouche, A. Le Beulze, J. C. Dupin, J. B. Ledeuil, S. Blanc, and D. Gonbeau, "Hybrid spiropyran-silica nanoparticles with a core-shell structure: sol-gel synthesis and photochromic properties," *Journal of Materials Chemistry*, vol. 20, no. 42, pp. 9370–9378, 2010.

[20] D. Jin, X. Miu, X. Yu, L. Wang, N. Wang, and L. Wang, "Synthesis of core-shell microspheres of poly(methyl methacrylate)-CuO by solution deposition method," *Materials Chemistry and Physics*, vol. 124, no. 1, pp. 69–72, 2010.

[21] V. A. Bershtein, V. M. Gun'ko, L. M. Egorova et al., "Well-defined oxide core-polymer shell nanoparticles: interfacial interactions, peculiar dynamics, and transitions in polymer nanolayers," *Langmuir*, vol. 26, no. 13, pp. 10968–10979, 2010.

[22] X. Chen, Z. Zhou, W. Lv, T. Huang, and S. Hu, "Preparation of core-shell structured T-ZnOw/polyaniline composites via graft polymerization," *Materials Chemistry and Physics*, vol. 115, no. 1, pp. 258–262, 2009.

[23] G. A. Buxton and N. Clarke, "Drug diffusion from polymer core-shell nanoparticles," *Soft Matter*, vol. 3, no. 12, pp. 1513–1517, 2007.

[24] J. Jang and Y. Kim, "Fabrication of monodisperse silica-polymer core-shell nanoparticles with excellent antimicrobial efficacy," *Chemical Communications*, no. 34, pp. 4016–4018, 2008.

[25] Y. K. Hwang, U. Jeong, and E. C. Cho, "Production of uniform-sized polymer core-shell microcapsules by coaxial electrospraying," *Langmuir*, vol. 24, no. 6, pp. 2446–2451, 2008.

[26] H. Zou, S. Wu, and J. Shen, "Preparation of silica-coated poly(styrene-co-4-vinylpyridine) particles and hollow particles," *Langmuir*, vol. 24, no. 18, pp. 10453–10461, 2008.

[27] A. R. Mahdavian, M. Ashjari, and H. S. Mobarakeh, "Nanocomposite particles with core-shell morphology—I. Preparation and characterization of Fe_3O_4-poly(butyl acrylate-styrene) particles via miniemulsion polymerization," *Journal of Applied Polymer Science*, vol. 110, no. 2, pp. 1242–1249, 2008.

[28] H. Y. Lee, S. P. Rwei, L. Wang, and P. H. Chen, "Preparation and characterization of core-shell polyaniline-polystyrene sulfonate@Fe_3O_4 nanoparticles," *Materials Chemistry and Physics*, vol. 112, no. 3, pp. 805–809, 2008.

[29] X. Liu, H. Wu, F. Ren, G. Qiu, and M. Tang, "Controllable fabrication of SiO_2/polypyrrole core-shell particles and polypyrrole hollow spheres," *Materials Chemistry and Physics*, vol. 109, no. 1, pp. 5–9, 2008.

[30] S. Sacanna and A. P. Philipse, "A generic single-step synthesis of monodisperse core/shell colloids based on spontaneous pickering emulsification," *Advanced Materials*, vol. 19, no. 22, pp. 3824–3826, 2007.

[31] A. Schmid, S. Fujii, S. P. Armes et al., "Polystyrene-silica colloidal nanocomposite particles prepared by alcoholic dispersion polymerization," *Chemistry of Materials*, vol. 19, no. 10, pp. 2435–2445, 2007.

[32] D. Duping, A. Schmidt, J. A. Balmer, and S. P. Armes, "Efficient synthesis of poly(2-vinylpyridine)-silica colloidal nanocomposite particles using a cationic azo initiator," *Langmuir*, vol. 23, no. 23, pp. 11812–11818, 2007.

[33] Y. P. Zhang, S. H. Lee, K. R. Reddy, A. I. Gopalan, and K. P. Lee, "Synthesis and characterization of core-shell SiO_2 nanoparticles/poly(3-aminophenylboronic acid) composites," *Journal of Applied Polymer Science*, vol. 104, no. 4, pp. 2743–2750, 2007.

[34] X. Ye, Y. Zhou, J. Chen, and Y. Sun, "Synthesis and infrared emissivity study of collagen-g-PMMA/Ag@TiO_2 composite," *Materials Chemistry and Physics*, vol. 106, no. 2-3, pp. 447–451, 2007.

[35] J. Jang, J. Ha, and B. Lim, "Synthesis and characterization of monodisperse silica-polyaniline core-shell nanoparticles," *Chemical Communications*, no. 15, pp. 1622–1624, 2006.

[36] G. Qiu, Q. Wang, and M. Nie, "Polyaniline/Fe_3O_4 magnetic nanocomposite prepared by ultrasonic irradiation," *Journal of Applied Polymer Science*, vol. 102, no. 3, pp. 2107–2111, 2006.

[37] P. Liu, L. Zhang, and Z. Su, "Core/shell SiOx@PAM nanospheres from UV-assisted surface-initiated free radical polymerization," *Journal of Applied Polymer Science*, vol. 100, no. 5, pp. 3433–3438, 2006.

[38] L. Wang, J. Hu, H. Zhang, and T. Zhang, "Au-impregnated polyacrylonitrile (PAN)/polythiophene (PTH) core-shell nanofibers with high-performance semiconducting properties," *Chemical Communications*, vol. 47, no. 24, pp. 6837–6839, 2011.

[39] W. Wu, T. Zhou, A. Berliner, P. Banerjee, and S. Zhou, "Smart core-shell hybrid nanogels with ag nanoparticle core for cancer cell imaging and gel shell for pH-regulated drug delivery," *Chemistry of Materials*, vol. 22, no. 6, pp. 1966–1976, 2010.

[40] J. Tian, J. Jin, F. Zheng, and H. Zhao, "Self-assembly of gold nanoparticles and polystyrene: a highly versatile approach to the preparation of colloidal particles with polystyrene cores and gold nanoparticle coronae," *Langmuir*, vol. 26, no. 11, pp. 8762–8768, 2010.

[41] J. C. Boyer, M. P. Manseau, J. I. Murray, and F. C. J. M. Van Veggel, "Surface modification of upconverting $NaYF_4$ nanoparticles with PEG-phosphate ligands for NIR (800 nm) biolabeling within the biological window," *Langmuir*, vol. 26, no. 2, pp. 1157–1164, 2010.

[42] J. C. Meredith, J. H. Lee, M. A. Mahmoud, V. B. Sitterle, and J. J. Sitterle, "Highly scattering, surface-enhanced raman scattering-active, metal nanoparticle-coated polymers prepared via combined swelling—Heteroaggregation," *Chemistry of Materials*, vol. 21, no. 23, pp. 5654–5663, 2009.

[43] A. S. Kumbhar and G. Chumanov, "Encapsulation of silver nanoparticles into polystyrene microspheres," *Chemistry of Materials*, vol. 21, no. 13, pp. 2835–2839, 2009.

[44] W. Wu, T. Zhou, and S. Zhou, "Tunable photoluminescence of Ag nanocrystals in multiple-sensitive hybrid microgels," *Chemistry of Materials*, vol. 21, pp. 2851–2861, 2009.

[45] S. Xing, L. H. Tan, M. Yang et al., "Highly controlled core/shell structures: tunable conductive polymer shells on gold nanoparticles and nanochains," *Journal of Materials Chemistry*, vol. 19, no. 20, pp. 3286–3291, 2009.

[46] A. Ohnuma, E. C. Cho, M. Jiangs, B. Ohtani, and Y. Xia, "Metal-polymer hybrid colloidal particles with an eccentric structure," *Langmuir*, vol. 25, no. 24, pp. 13880–13887, 2009.

[47] S. Xuan, Y. X. J. Wang, J. C. Yu, and K. C. F. Leung, "Preparation, characterization, and catalytic activity of core/shell Fe_3O_4@polyaniline@Au nanocomposites," *Langmuir*, vol. 25, no. 19, pp. 11835–11843, 2009.

[48] S. R. Guo, J. Y. Gong, P. Jiang, M. Wu, Y. Lu, and S. H. Yu, "Biocompatible luminescent silver@phenol formaldehyde resin core/shell nanospheres: narge-ncale synthesis and application for in vivo bioimaging," *Advanced Functional Materials*, vol. 18, pp. 872–879, 2008.

[49] B. Yin and M. Hakkarainen, "Core-shell nanoparticle-plasticizers for design of high-performance polymeric materials with improved stiffness and toughness," *Journal of Materials Chemistry*, vol. 21, pp. 8670–8677, 2011.

[50] M. G. Han, J. Sperry, A. Gupta, C. F. Huebner, S. T. Ingram, and S. H. Foulger, "Polyaniline coated poly(butyl methacrylate) core-shell particles: roll-to-roll printing of templated electrically conductive structures," *Journal of Materials Chemistry*, vol. 17, no. 14, pp. 1347–1352, 2007.

[51] J. L. Zhang, R. S. Srivastava, and R. D. K. Misra, "Core-shell magnetite nanoparticles surface encapsulated with smart stimuli-responsive polymer: synthesis, characterization, and LCST of viable drug-targeting delivery system," *Langmuir*, vol. 23, no. 11, pp. 6342–6351, 2007.

[52] H. Zhang, X. Zhong, J. J. Xu, and H. Y. Chen, "Fe_3O_4/Polypyrrole/Au nanocomposites with core/shell/shell structure: synthesis, characterization, and their electrochemical properties," *Langmuir*, vol. 24, no. 23, pp. 13748–13752, 2008.

[53] G. Gonalves, P. A. A. P. Marques, A. Barros-Timmons et al., "Graphene oxide modified with PMMA via ATRP as a reinforcement filler," *Journal of Materials Chemistry*, vol. 20, no. 44, pp. 9927–9934, 2010.

[54] K. Y. Pu, K. Li, J. Shi, and B. Liu, "Fluorescent single-molecular core-shell nanospheres of hyperbranched conjugated polyelectrolyte for live-cell imaging," *Chemistry of Materials*, vol. 21, no. 16, pp. 3816–3822, 2009.

[55] B. Yuan and D. A. Wicks, "Thermotropic color changing nanoparticles prepared by encapsulating blue polystyrene particles with a poly-N-isopropylacrylamide gel," *Journal of Applied Polymer Science*, vol. 105, no. 2, pp. 446–452, 2007.

[56] D. Li, B. Dong, X. Bai, Y. Wang, and H. Song, "Influence of the TGA modification on upconversion luminescence of hexagonal-phase $NaYF_4$:Yb^{3+}, Er^{3+} nanoparticles," *Journal of Physical Chemistry C*, vol. 114, no. 18, pp. 8219–8226, 2010.

[57] H. Chen, X. Wu, H. Duan et al., "Biocompatible polysiloxane-containing diblock copolymer PEO-b-PγMPS for coating magnetic nanoparticles," *ACS Applied Materials & Interfaces*, vol. 1, no. 10, pp. 2134–2140, 2009.

[58] J. Han, Y. Liu, and R. Guo, "A simple one-step chemical route to gold/polymer core/shell composites and polymer hollow spheres," *Journal of Applied Polymer Science*, vol. 112, no. 3, pp. 1244–1249, 2009.

[59] F. Wen, W. Zhang, G. Wei et al., "Synthesis of noble metal nanoparticles embedded in the shell layer of core-shell poly(styrene-co-4-vinylpyridine) micospheres and their application in catalysis," *Chemistry of Materials*, vol. 20, no. 6, pp. 2144–2150, 2008.

[60] X. Jiang and J. Yin, "Photoinitiated synthesis of polymer brush from dendritic photoinitiator electrostatic self-assembly," *Chemical Communications*, no. 39, pp. 4927–4928, 2005.

[61] A. W. Green, A. W. Timms, and P. N. Green, in *Proceedings of Radtecheurope*, p. 636, RadTechEurope, Fribourg, Switzerland, Edinburgh, Scotland, 1991.

[62] W. Stöber, A. Fink, and E. Bohn, "Synthesis of silica nanoparticles," *Journal of Colloid and Interface Science*, vol. 26, pp. 62–66, 1968.

[63] L. Liu, B. Li, R. Qin, H. Zhao, X. Ren, and Z. Su, "Synthesis and characterization of new bifunctional nanocomposites possessing upconversion and oxygen-sensing properties," *Nanotechnology*, vol. 21, no. 28, Article ID 285701, 2010.

[64] G. Chen, H. Liu, H. Liang, G. Somesfalean, and Z. Zhang, "Upconversion emission enhancement in Yb^{3+}/Er^{3+}-codoped Y_2O_3 nanocrystals by tridoping with Li^+ ions," *Journal of Physical Chemistry C*, vol. 112, no. 31, pp. 12030–12036, 2008.

[65] Z. Li, L. A. Fredin, P. Tewari et al., "In situ catalytic encapsulation of core-shell nanoparticles having variable shell thickness: dielectric and energy storage properties of high-permittivity metal oxide nanocomposites," *Chemistry of Materials*, vol. 22, pp. 5154–5164, 2010.

[66] N. V. Long, T. D. Hien, T. Asaka, M. Ohtaki, and M. Nogami, "Synthesis and characterization of Pt-Pd alloy and core-shell bimetallic nanoparticles for direct methanol fuel cells (DMFCs): enhanced electrocatalytic properties of well-shaped core-shell morphologies and nanostructures," *International Journal of Hydrogen Energy*, vol. 36, no. 14, pp. 8478–8491, 2011.

[67] A. Alonso, A. Macanás, A. Shafir et al., "Donnan-exclusion-driven distribution of catalytic ferromagnetic nanoparticles synthesized in polymeric fibers," *Dalton Transactions*, vol. 39, pp. 2579–2586, 2010.

[68] S. Wei, Q. Wang, J. Zhu et al., "Multifunctional composite core-shell nanoparticles ," *Nanoscale*, vol. 3, pp. 4474–4502, 2011.

[69] J. Zhu, S. Wei, N. Haldolaarachchige, D. P. Young, and Z. Gou, "Electromagnetic field shielding polyurethane nanocomposites reinforced with core-shell Fe-Silica nanoparticles," *The Journal of Physical Chemistry C*, vol. 115, pp. 15304–15310, 2011.

[70] J. Zhu, S. Wei, I. Y. Lee et al., "Silica stabilized iron particles toward anti-corrosion magnetic polyurethane nanocomposites," *RSC Advances*, vol. 2, pp. 1136–1143, 2012.

[71] J. Zhu, S. Wei, H. Gu et al., "One-pot synthesis of magnetic graphene nanocomposites decorated with core@double-shell nanoparticles for fast chromium removal," *Environmental Science and Technology*, vol. 46, pp. 977–985, 2012.

[72] H. Gu, Y. Huang, X. Zhang et al., "Magnetoresistive polyaniline-magnetite nanocomposites with negative dielectrical properties," *Polymer*, vol. 53, pp. 801–809, 2012.

[73] Z. Guo, C. S. S. R. Kumar, L. L. Henry et al., "Displacement synthesis of Cu shells surrounding Co nanoparticles," *Journal of Electrochemical Society*, vol. 1, pp. D1–D5, 2005.

[74] Z. Guo, L. L. Henry, and E. J. Podlaha, "An examination of Co and Fe core nanoparticles with a protecting shell," *ECS Transactions*, vol. 1, pp. 63–69, 2006.

[75] Z. Guo, L. L. Henry, and E. J. Podlaha, "CoFe, Fe and Co nanoparticle displacement with Cu ions," *ECS Transactions*, vol. 3, pp. 337–345, 2007.

[76] B. Guo, W. A. Finne, and A. C. Albertsson, "Simple route to size-tunable degradable and electroactive nanoparticles from the self-assembly of conducting coil rod coiltriblock copolymers," *Chemistry of Materials*, vol. 23, pp. 4045–4055, 2011.

[77] X. Yang, L. Chen, B. Huang, F. Bai, and X. Yang, "Synthesis of pH-sensitive hollow polymer microspheres and their application as drug carriers," *Polymer*, vol. 50, no. 15, pp. 3556–3563, 2009.

[78] G. A. Buxton and C. Nigel, "Drug diffusion from polymer core-shell nanoparticles," *Soft Matter*, vol. 3, pp. 1513–1517, 2007.

[79] D. Lina, J. Yiguang, Y. Jiangyong et al., "A functionalized poly(amidoamine) nanocarrier-loading 5-fluorouracil: pH-responsive drug release and enhanced anticancer effect," *Anti-Cancer Drugs*, vol. 24, pp. 172–180, 2013.

[80] K. R. Reddy, K. P. Lee, J. Y. Kim, and Y. Lee, "Self-assembly and graft polymerization route to monodispersed Fe_3O_4@SiO_2-polyaniline core-shell composite nanoparticles: physical properties," *Journal of Nanoscience and Nanotechnology*, vol. 8, no. 11, pp. 5632–5639, 2008.

[81] C. Sun, J. S. H. Lee, and M. Zhang, "Magnetic nanoparticles in MR imaging and drug delivery," *Advanced Drug Delivery Reviews*, vol. 60, pp. 1252–1265, 2008.

[82] N. Nishiyama and K. Kataoka, "Nanostructured devices based on block copolymer assemblies for drug delivery: designing structures for enhanced drug function," *Advances in Polymer Science*, vol. 193, no. 1, pp. 67–101, 2006.

[83] J. Wu and A. Eisenberg, "Proton diffusion across membranes of vesicles of poly(styrene-b-acrylic acid) diblock copolymers," *Journal of the American Chemical Society*, vol. 128, no. 9, pp. 2880–2884, 2006.

[84] D. A. Tomalia, "Birth of a new macromolecular architecture: dendrimers as quantized building blocks for nanoscale synthetic polymer chemistry," *Progress in Polymer Science*, vol. 30, no. 3-4, pp. 294–324, 2005.

[85] O. C. Farokhzad, J. Cheng, B. A. Teply et al., "Targeted nanoparticle-aptamer bioconjugates for cancer chemotherapy in vivo," *Proceedings of the National Academy of Sciences of the United States of America*, vol. 103, no. 16, pp. 6315–6320, 2006.

[86] V. Yathindranath, T. Hegmann, J. Van Lierop, K. Potter, C. B. Fowler, and D. F. Moore, "Simultaneous magnetically directed drug convection and MR imaging," *Nanotechnology*, vol. 20, no. 40, Article ID 405101, 2009.

[87] F. Yu, L. Zhang, Y. Huang, K. Sun, A. E. David, and V. C. Yang, "The magnetophoretic mobility and superparamagnetism of core-shell iron oxide nanoparticles with dual targeting and imaging functionality," *Biomaterials*, vol. 31, no. 22, pp. 5842–5848, 2010.

[88] M. Wang, C. C. Mi, W. X. Wang et al., "Immunolabeling and NIR-excited fluorescent imaging of HeLa cells by using $NaYF_4$:Yb,Er upconversion nanoparticles," *ACS Nano*, vol. 3, no. 6, pp. 1580–1586, 2009.

[89] Y. Lu, S. Proch, M. Schrinner, M. Drechsler, R. Kempe, and M. Ballauff, "Thermosensitive core-shell microgel as a "nanoreactor" for catalytic active metal nanoparticles," *Journal of Materials Chemistry*, vol. 19, pp. 3955–3961, 2009.

[90] T. Chen, P. Xu, Y. Luo et al., "Preparation of poly(butyl acrylate)-poly(methyl methacrylate) (core-shell)/phosphor composite particles and its application in PVC matrix," *Journal of Applied Polymer Science*, vol. 114, no. 1, pp. 496–502, 2009.

[91] H. Takahashi, T. Niidome, T. Kawano, S. Yamada, and Y. Niidome, "Surface modification of gold nanorods using layer-by-layer technique for cellular uptake," *Journal of Nanoparticle Research*, vol. 10, no. 1, pp. 221–228, 2008.

[92] Z. Liao, H. Wang, R. Lv et al., "Polymeric liposomes-coated superparamagnetic iron oxide nanoparticles as contrast agent for targeted magnetic resonance imaging of cancer cells," *Langmuir*, vol. 27, no. 6, pp. 3100–3105, 2011.

[93] M. Gonzales-Weimuller, M. Zeisberger, and K. M. Krishnan, "Size-dependant heating rates of iron oxide nanoparticles for magnetic fluid hyperthermia," *Journal of Magnetism and Magnetic Materials*, vol. 321, no. 13, pp. 1947–1950, 2009.

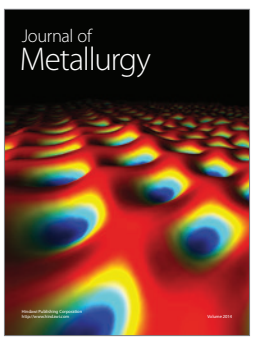

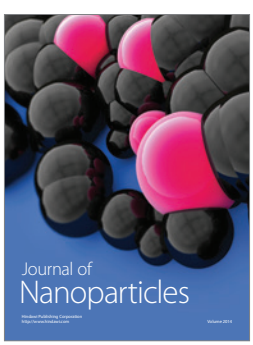

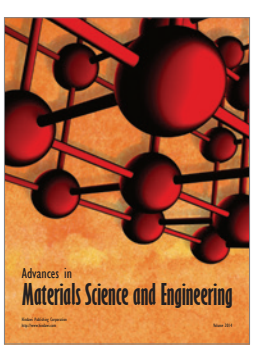

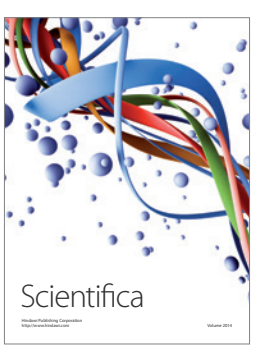

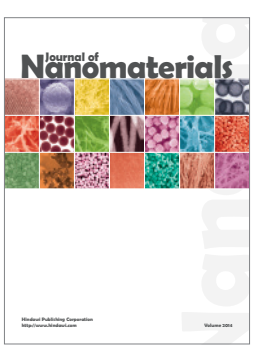

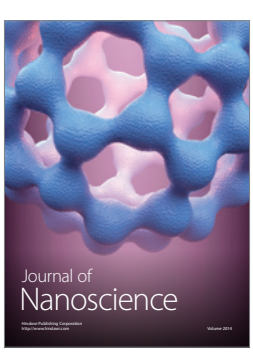

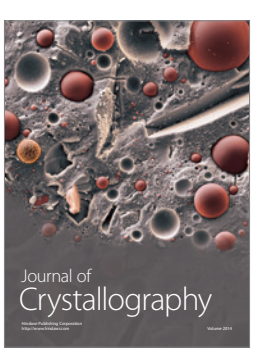

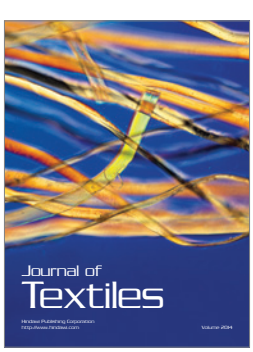

Hindawi

Submit your manuscripts at
http://www.hindawi.com